RESEARCH PAPER

BJP | BRITISH PHARMACOLOGICAL SOCIETY

# nNOS-CAPON blockers produce anxiolytic effects by promoting synaptogenesis in chronic stress-induced animal models of anxiety

Li-Juan Zhu[1]  |  Hu-Jiang Shi[1]  |  Lei Chang[2]  |  Cheng cheng Zhang[1]  |  Meng Si[3]  |  Na Li[1]  |  Dong-Ya Zhu[2]

[1]Key Laboratory of Developmental Genes and Human Diseases, MOE, Department of Histology and Embryology, School of Medicine, Southeast University, Nanjing, Jiangsu, China

[2]Department of Pharmacology, School of Pharmacy, Nanjing Medical University, Nanjing, Jiangsu, China

[3]The First Affiliated Hospital of USTC, Division of Life Sciences and Medicine, University of Science and Technology of China, Hefei, Anhui, China

**Correspondence**
Li-Juan Zhu, Key Laboratory of Developmental Genes and Human Diseases, MOE, Department of Histology and Embryology, School of Medicine, Southeast University, Nanjing, Jiangsu 210009, China.
Email: lijuan_zhu2004@126.com

Dong-Ya Zhu, Department of Pharmacology, School of Pharmacy, Nanjing Medical University, Nanjing, Jiangsu 211166, China.
Email: dyzhu@njmu.edu.cn

**Background and Purpose:** Anxiety disorder is a common mental health disorder. However, there are few safe and fast-acting anxiolytic drugs available that can treat anxiety disorder. We previously demonstrated that the interaction of neuronal NOS (nNOS) with its carboxy-terminal PDZ ligand (CAPON) is involved in regulating anxiety-related behaviours. Here, we further investigated the anxiolytic effects of nNOS–CAPON disruptors in chronic stress-induced anxiety in animals.

**Experimental Approach:** Mice were intravenously treated with nNOS–CAPON disruptors, ZLc-002 or Tat-CAPON12C, at the last week of chronic mild stress (CMS) exposure. We also infused corticosterone (CORT) into the hippocampus of mice to model anxiety behaviours and also delivered ZLc-002 or Tat-CAPON12C on the last week of chronic CORT treatment via pre-implanted cannula. Anxiety-related behaviours were examined using elevated plus maze, open field, novelty-suppressed feeding and light–dark (LD) tests. The level of nNOS–CAPON interaction was determined by co-immunoprecipitation (CO-IP) and proximity ligation assay (PLA). The neural mechanisms underlying the behavioural effects of nNOS–CAPON uncoupling in anxiety animal models were assessed by western blot, immunofluorescence and Golgi-Cox staining.

**Key Results:** ZLc-002 and Tat-CAPON12C reversed CMS- or CORT-induced anxiety-related behaviours. ZLc-002 and Tat-CAPON12C increased synaptogenesis along with improved dendritic remodelling in CMS mice or CORT-treated cultured neurons. Meanwhile, blocking nNOS–CAPON interaction significantly activated the cAMP response element-binding protein (CREB)–brain-derived neurotrophic factor (BDNF) pathway, which is associated with synaptic plasticity.

**Conclusion and Implications:** Collectively, these results provide evidence for the anxiolytic effects of nNOS–CAPON uncouplers and their underlying mechanisms in anxiety disorders.

---

**Abbreviations:** BDNF, brain-derived neurotrophic factor; BZDs, benzodiazepines; CAPON, carboxyl-terminal PDZ ligand of neuronal nitric oxide synthase protein; CMS, chronic mild stress; CO-IP, coimmunoprecipitation; CORT, corticosterone; CREB, cAMP response element-binding protein; Dexras1, dexamethasone-induced ras protein 1; DG, dentate gyrus; eNOS, endothelial NOS; EPM, elevated plus maze; ERK, extracellular regulated protein kinases; iNOS, inducible NOS; LD, light–dark; nNOS, neuronal NOS; NSF, novelty-suppressed feeding; OF, open field; PLA, proximity ligation assay; RRID, research resource identifier; SSRIs, selective serotonin reuptake inhibitors.

# 1 | INTRODUCTION

Anxiety disorder, also known as anxiety neurosis, is the most common type of neurosis. Severe anxiety can lead to attempted suicide or suicidal behaviours (Crocq, 2017; Hawgood & De Leo, 2008; Sareen et al., 2005). At present, the main drugs for treating anxiety are selective serotonin reuptake inhibitors (SSRIs) and benzodiazepines (BZDs). However, the former has a slow onset and is ineffective in some patients, while the latter has a number of side effects and poor safety (Cryan & Sweeney, 2011; Farb & Ratner, 2014). Little is known about the pathogenesis of anxiety disorders and unfortunately, there are few safe and fast-acting therapeutic drugs for key pathological mechanisms involved. Therefore, in-depth exploration of the control mechanism of anxiety is of great significance for developing new anxiolytics.

Our previous studies have shown that hippocampal neuronal NOS (**nNOS**) plays an important role in regulating anxiety behaviour. In particular, hippocampal nNOS– Ccarboxyl-terminal PDZ ligand of neuronal nitric oxide synthase protein (CAPON) coupling may serve as a new target for developing potential anxiolytics (Hu et al., 2012; Zhu et al., 2014; Zhu et al., 2018). Fortunately, among the many nNOS–CAPON blockers that we have designed and synthesised, ZLc-002 and Tat-CAPON12C have significant anxiolytic-like effects (Zhu et al., 2014). Additionally, we also found that ZLc-002 was a rapid-onset pro-drug without sedative, myorelaxant or incoordination effects. Although we have demonstrated that nNOS–CAPON blockers have significant anxiolytic-like effects under physiological conditions, it is worthwhile to study whether nNOS–CAPON blockers have anxiolytic effects in chronic stress-induced anxiety in animals, especially when the blockers were administered after the onset of anxious behaviours.

An increasing number of studies have found that hippocampal synaptic plasticity alterations are associated with affective disorders such as anxiety (Bannerman et al., 2014). Interestingly, our previous results showed that **dexamethasone**-induced ras protein 1 (Dexras1)–ERK signalling and hippocampal synaptic plasticity were involved in the anxiety-related behavioural effects of hippocampal nNOS–CAPON association (Zhu et al., 2014). However, the mechanisms by which nNOS–CAPON blockers exert an anxiolytic effect on anxiety animal models are not clear. In this study, we explored the anxiolytic effects and underlying neural mechanisms of nNOS–CAPON blockers on chronic stress-induced anxiety animal models and found that both ZLc-002 and Tat-CAPON12C treatments reversed the anxiogenic behaviours induced by chronic mild stress (CMS) or chronic corticosteroids exposure, especially in the late stages. Meanwhile, nNOS–CAPON blockers reversed the impairment in synaptogenesis, dendritic outgrowth and cAMP response element-binding protein (CREB)–brain-derived neurotrophic factor (**BDNF**) pathway induced by chronic stress *in vivo* and *in vitro*. Therefore, our work presents that nNOS–CAPON blockers may serve as potential and promising anxiolytics.

---

**What is already known**

- nNOS–CAPON blockers have significant anxiolytic-like effects under physiological conditions.

**What this study adds**

- nNOS–CAPON blockers have anxiolytic effects in chronic stress-induced anxiety in animals through neuroplasticity up-regulation.

**What is the clinical significance**

- nNOS–CAPON blockers may serve as potential and promising anxiolytics.

---

# 2 | METHODS

## 2.1 | Animals

Young adult (6–7 weeks) male homozygous nNOS-knockout mice (B6; 129S4-Nos1 tm1Plh, stock number: 002633) and the wild-type controls of similar genetic backgrounds (B6129SF2, WT) (both from Jackson Laboratories, maintained at Model Animal Research Centre of Nanjing University, Nanjing, China), and young adult (6–7 weeks, 22–28 g) ICR male mice and newborn (postnatal day P0–P1) ICR mice (RRID:IMSR_RBRC05979) (from Model Animal Research Centre of Nanjing University, Nanjing, China) were used in this study. Animals were maintained at a controlled temperature (20 ± 2°C) and housed (12-h light/dark cycle) with access to food and water ad libitum, except when specified otherwise. Every effort was made to minimise the number of animals used and their suffering. All procedures involving the use of animals were approved by the Institutional Animal Care and Use Committee of Southeast University (IACUC-20160710003). Animals were killed by administering isoflurane as an anaesthetic followed by decapitation as a confirmation method. No animals were excluded from the statistical analysis. Animal studies are reported in compliance with the ARRIVE guidelines (Kilkenny, Browne, Cuthill, Emerson, & Altman, 2010) and with the recommendations made by the *British Journal of Pharmacology*.

## 2.2 | Drugs and intrahippocampal infusions

ZLc-002, a small molecular inhibitor of nNOS–CAPON interaction, was designed and synthesised in our laboratory (Zhu et al., 2014). Tat-

CAPON12C (YGRKKRRQRRRELGDSLDDEIAV), a recombinant fusion protein with the action to dissociate nNOS–CAPON, and its control peptide Tat-CAPON12C/A22D (YGRKKRRQRRRELGDSLDDEIDV) were purchased from Shanghai GL Biochem Ltd. ZLc-002 and Tat-CAPON12C were dissolved in 0.9% sterile saline and corticosterone (CORT, Cat# 27840, Sigma-Aldrich, St Louis, MO, USA) in 0.1% DMSO. Corticosterone (10 μM), ZLc-002 (10 μM) and Tat-CAPON12C (50 nM) were delivered into the dentate gyrus (DG) of the hippocampus by microinjection through a pre-implanted cannula as described previously (Zhu et al., 2018). In brief, mice were anaesthetised with 2% isoflurane and maintained under 1.5%–2.0% isoflurane. Drug treatment experiments were performed in the animal centre between 9 and 11 a.m.

## 2.3 | Experimental protocols and design

In this study, adult male ICR mice were used in experiments 1 and 2. Newborn (postnatal day P0–P1) ICR mice were used for primary neuronal cultures and young adult male homozygous nNOS-knockout mice as well as wild-type controls of a similar genetic background for the biochemical analysis in experiment 3. The investigators were blinded to the treatments. All the adult mice were numbered using earmarks and were randomly divided into groups with equal size using a table of random numbers.
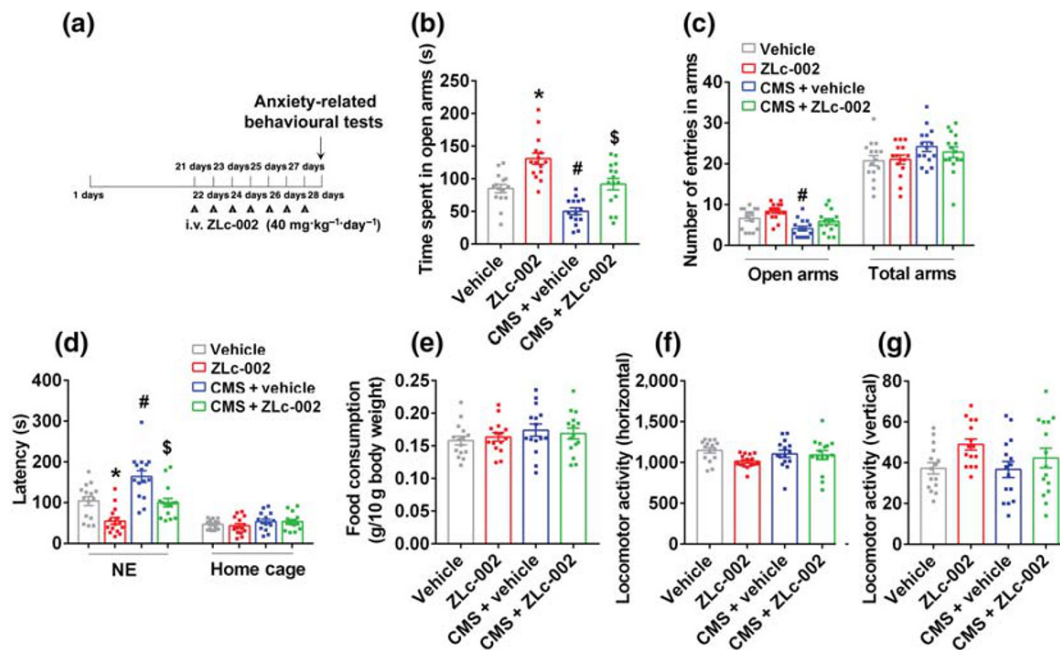
### 2.3.1 | Experiment 1

This experiment was performed to determine the anxiolytic effects of nNOS–CAPON blockers in a chronic mild stress-induced anxiety animal model. (1) Mice were randomly divided into four groups, including the vehicle, ZLc-002, chronic mild stress + vehicle and chronic mild stress + ZLc-002 groups. Each group consisted of 15 animals. (2) Mice were randomly divided into four groups, including Tat-CAPON12C/A22D, Tat-CAPON12C, chronic mild stress + Tat-CAPON12C/A22D and chronic mild stress + Tat-CAPON12C groups, with 15 animals each. Two mice in the chronic mild stress + Tat-CAPON12C/A22D- or chronic mild stress + Tat-CAPON12C-treated group died after chronic mild stress exposure. (3) Mice were then randomly divided into three groups, including vehicle, chronic mild stress + vehicle and chronic mild stress + Tat-CAPON12C/A22D groups, with 13 animals each. ZLc-002 (40 mg·kg$^{-1}$·day$^{-1}$) or vehicle, Tat-CAPON12C (3 μmol·kg$^{-1}$·day$^{-1}$) or its control peptide Tat-CAPON12C/A22D (3 μmol·kg$^{-1}$·day$^{-1}$) was administered intravenously between day 21 and day 27 of chronic mild stress exposure. Twenty-four hours after the last treatment, their behaviours were examined, the hippocampi were immediately isolated for further biochemical analysis, and the brains were taken for histological analysis. The investigators involved in the data analysis were blinded to the sample identity. The detailed experimental procedure can be found in Figures 1, 2 and S2.

### 2.3.2 | Experiment 2

This experiment was designed to examine the effect of nNOS–CAPON blockers on glucocorticoid-induced anxiogenic behaviours. (1) The mice were randomly divided into three groups:- vehicle, corticosterone + vehicle and corticosterone + ZLc-002 groups, with 11 animals each. (2) The mice were randomly divided into three groups: Tat-CAPON12C/A22D, corticosterone + Tat-CAPON12C/A22D and corticosterone + Tat-CAPON12C groups, with 11 animals each. (3) The mice were randomly divided into four groups:- vehicle, ZLc-002, Tat-CAPON12C/A22D and Tat-CAPON12C groups, with 14 animals each. (4) The mice were randomly divided into three groups: vehicle, corticosterone + vehicle and corticosterone + Tat-CAPON12C/A22D groups, with 13 animals each. Corticosterone (10 μM) or its vehicle was delivered into the dentate gyrus of the hippocampus daily using a microinjection through a pre-implanted cannula (30 gauge, 4.0 mm; RWD Life Science Co., Ltd) terminating 0.50 mm below the tip of the guides and connected by polyethylene tubing (PE-10) to a 10-μl Hamilton syringe. The administration was controlled by an infusion pump programmed to deliver a volume of 1 μl at a flow-rate of 0.1 μl·min$^{-1}$, as described previously (Zhu et al., 2018). ZLc-002 (10 μM, 1 μl, administrated 30 min after corticosterone), Tat-CAPON12C (50 nM, 1 μl, administrated 30 min after corticosterone), its vehicle or control peptide was infused into the hippocampus between day 21 and day 27 of corticosterone(10 μM, 1 μl) treatment via a pre-implanted cannula. Their behaviours were examined 24 h after the last treatments. After completion of the behavioural tests, the precision of the coordinates for the local infusion of dentate gyrus was validated using a microinjection of DiIC18 (3) (DiI), a red colour dye, into the dentate gyrus (Figure S1A). The investigators involved in the data analysis were blinded to the sample identity.

### 2.3.3 | Experiment 3

This experiment was performed to explore the underlying neural mechanism of anxiolytic effects exerted by nNOS–CAPON blockers in anxiety animal models. (1) Primary cultured hippocampal neurons were incubated with corticosterone (10 μM) with or without ZLc-002 (10 μM) for 72 h at 7 days in vitro. Cellular samples were collected for protein detection of PSD-95, synapsin, BDNF, CREB and phosphorylation of cAMP response element-binding protein (p-CREB). After PBS/PFA fixation, neurons were stored for proximity ligation assay (PLA). (2) Primary cultured hippocampal neurons were incubated with 10-μM corticosterone with or without 50-nM Tat-CAPON12C for 72 h at 7 days in vitro, and neurons were collected for further biochemical analysis. (3) Young adult male homozygous nNOS-knockout mice and the wild-type controls were administered with ZLc-002 (40 mg·kg$^{-1}$·day$^{-1}$) intravenously for 7 days. Twenty-four hours after the last treatment, the hippocampi were immediately isolated for further biochemical analysis.

**FIGURE 1** ZLc-002 attenuates chronic mild stress (CMS) -induced anxiogenic behaviour. (a) Diagram showing the design of the experiments in (b)–(g). The adult male ICR mice were treated with ZLc-002 (40 mg·kg$^{-1}$·day$^{-1}$) or its vehicle by intravenous administration for 7 consecutive days on 21 days after CMS exposure. (b) The time spent in open arms, and (c) number of entries in the arms in the elevated plus maze (EPM) test. (d) The latency to feed in a novel environment and in the home cage, and (e) food consumption in the home cage in the novelty-suppressed feeding (NSF) test. (f,g) The locomotor activity of mice in the open field (OF) test. Parameters for the locomotor activities were the number of square crossings (horizontal) and the time standing (vertical). Mean ± SEM, $n = 15$ mice in each group, $^*P < 0.05$, compared with vehicle-treated group; $^\#P < 0.05$, compared with vehicle-treated non-CMS group; $^\$P < 0.05$, compared with vehicle-treated CMS group, two-way ANOVA followed by Tukey's post-test (b–g). NE, novel environment; total arms, open arms + enclosed arms
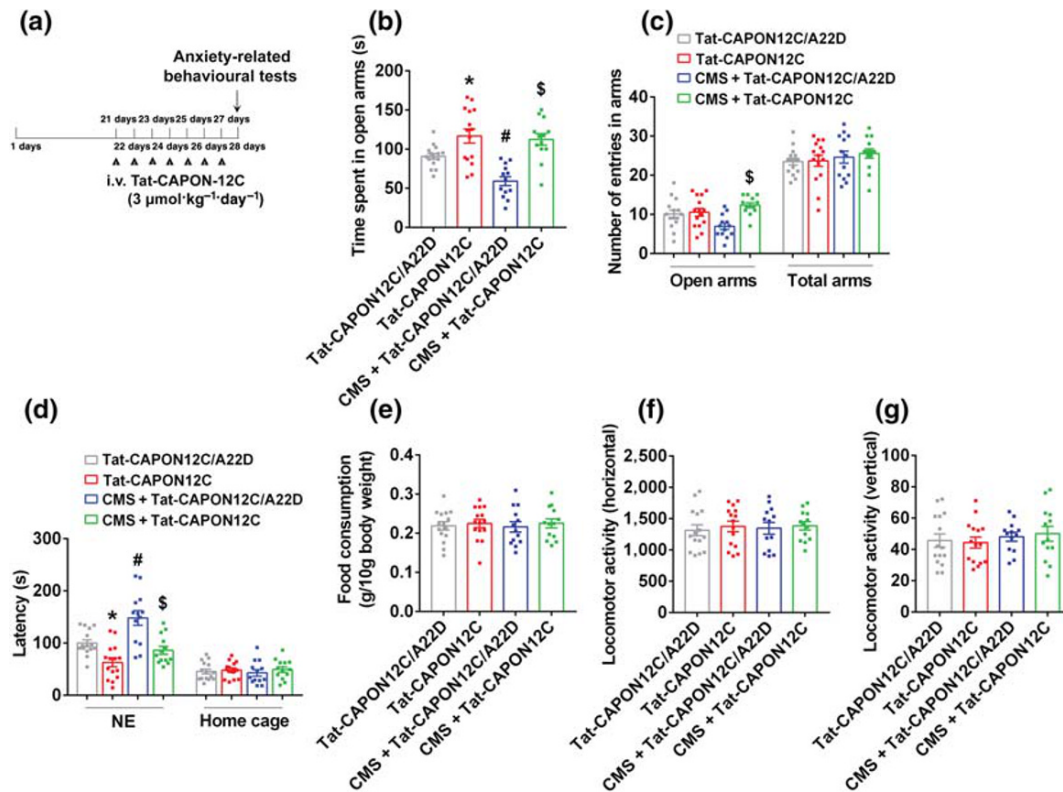
## 2.4 | Chronic mild stress

The chronic mild stress procedure was designed as described in our previous studies (Cai et al., 2019; Ducottet, Griebel, & Belzung, 2003; Zhang et al., 2010; Zhou et al., 2007; Zhu et al., 2018). It consisted of a variety of mild stressors (Table 1). The mice in the chronic mild stressgroup were exposed to the following stressors:- restraint, forced swimming, food/water deprivation, tilted cage (40° from horizontal), housed in wet sawdust and reversal of the light/dark cycle. chronic mild stress was conducted for 4 weeks for all stress groups.

## 2.5 | Behavioural tests

The behavioural tests were performed as described in our previous study (Zhang et al., 2010; Zhu et al., 2018), including novelty-suppressed feeding (NSF), as well as the elevated plus maze (EPM), the open field (OF) and light–dark (LD) tests. The NSF test was carried out over a 5-min period. The testing apparatus consisted of a plastic box (50 × 50 × 20 cm). The latency to feed in a novel environment in 5 min has been used as an index of anxiety-related behaviours. The latency to feed in 5 min and the amount of food consumed by the mouse in 15 min in the home cage were used as a control for appetite changes as a possible confounding factor. The elevated plus maze test was assessed using an apparatus consisting of two open arms

(30 × 5 cm), two enclosed arms (30 × 5 cm, with end and side walls 15 cm high) and a central connecting platform (5 × 5 cm). Each mouse was placed in the intersection of the four arms, facing an open arm and allowed to explore freely for 5 min. The time spent in the open arms was used as an index of anxiety-related behaviour and a total number of entries into the total (open + enclosed) arms as a general activity. For open field test, the test arena was constructed of a plastic plate (56.13 × 56.13 cm) and divided into 256 squares by lines drawn on the floor of the plate. It was surrounded by a 35.18-cm-high plastic wall. Each mouse was placed onto a corner square of the arena, facing the corner and allowed to explore the open field for 5 min per trial freely. The light–dark test was performed using an apparatus consisting of two glass boxes (27 × 21 × 24 cm) with an interconnecting grey plastic tunnel (7 × 10 cm). One of the boxes was painted black and was weakly lit by a red 25-W bulb (0 lx). The other box was lit by a 60-W desk lamp (400 lx) placed 30 cm above the box, providing the only laboratory illumination. The floor was lined into 9-cm squares. The mice were introduced into the black compartment and observed for 5 min. Latency to enter (all four paws) the lit compartment and the time spent in the lit compartment were recorded.

After each trial, the plate was cleaned with 70% EtOH. All measurements in the mice were taken approximately 24 h after the last injection of the drugs. During the experiments and analysis, the investigators were blinded to the treatment group. The mice were

**FIGURE 2** Tat-CAPON12C reverses chronic mild stress (CMS)-induced anxiogenic behaviour. (a) Diagram showing the design of the experiments in (b)–(g). The adult male ICR mice were treated with Tat-CAPON12C (3 μmol·kg$^{-1}$·day$^{-1}$) or its control peptide Tat-CAPON12C/A22D by intravenous administration for 7 consecutive days on 21 days after CMS exposure. (b) The time spent in open arms, and (c) number of entries in the arms in the elevated plus maze (EPM) test. (d) The latency to feed in a novel environment and in the home cage, and (e) food consumption in the home cage in the novelty-suppressed feeding (NSF) test. (f–g) The locomotor activity of mice in the open field test. Parameters for the locomotor activities were the number of square crossings (horizontal) and the time standing (vertical). Mean ± SEM, Tat-CAPON12C/A22D or Tat-CAPON12C groups, $n = 15$ mice; CMS + Tat-CAPON12C/A22D or CMS + Tat-CAPON12C groups, $n = 13$ mice, $^*P < 0.05$, compared with Tat-CAPON12C/A22D-treated group; $^\#P < 0.05$, compared with Tat-CAPON12C/A22D-treated non-CMS group; $^\$P < 0.05$, compared with Tat-CAPON12C/A22D-treated CMS group, two-way ANOVA followed by Bonferroni's post hoc test (b–f). NE, novel environment; total arms, open arms + enclosed arms

identified using earmarks, and their numbers were given only after the behavioural experiments and analysis were completed.

## 2.6 | Culture of hippocampal neurons

Primary hippocampal neurons were cultured as reported previously (Zhang et al., 2010; Zhu et al., 2018). The planting density was $2 \times 10^4$ cells·cm$^{-2}$ for the morphological analysis and $1 \times 10^5$ cells·cm$^{-2}$ for the biochemical detection.

## 2.7 | Western blot analysis

Western blot analysis of samples from cultured hippocampal neurons and hippocampal tissues from animals was performed as described previously (Zhang et al., 2010; Zhou et al., 2007; Zhu et al., 2018). Briefly, the samples were lysed in ice-cold RIPA (Cat# P0013C, Beyotime Biotechnology, Shanghai, China). Protein concentrations were determined with the BCA Protein Assay Kit (Cat#23227,

Thermo Fisher Scientific, Waltham, MA, USA). The homogenates containing 15–20 μg of total protein were loaded on 8%–12% SDS-PAGE gels for electrophoresis followed by transferring to the PVDF membrane (Cat# ISEQ00010 for BDNF, Cat# IPVH00010 for other bands, Millipore Bioscience Research Reagents, Temecula, CA, USA). The membranes were blocked by 5% skimmed milk, and the primary antibodies were incubated overnight at 4°C, respectively, as follows: mouse anti-nNOS (1:1,000; Cat# 610308, RRID:AB_397700, BD Transduction Laboratories, Franklin Lakes, NJ, USA), rabbit anti-nNOS (1:2,000; Cat# AB5380, RRID:AB_91824, Millipore Bioscience Research Reagents, Temecula, CA, USA), rabbit anti-CAPON (1:10,000; Cat# ab190686, RRID:AB_2713895, Abcam, MA, USA), mouse anti-PSD-95 (1:10,000; Cat# ab2723, RRID:AB_303248, Abcam), rabbit anti-synapsin (1:4,000; Cat# AB1543P, RRID: AB_90757, Millipore Bioscience Research Reagents), mouse anti-BDNF (1:500, Cat# ab203573, RRID:AB_2631315, Abcam), rabbit anti-CREB (1:2,000; Cat# 9197, RRID:AB_331277, Cell Signaling Technology, Beverly, MA, USA) and rabbit anti-phospho-CREB-Ser133 (1:1,000; Cat# 9198, RRID:AB_2561044, Cell Signaling Technology). Internal control was performed using rabbit anti-GAPDH

**TABLE 1** Chronic mild stress (CMS) weekly schedule

| Week | | Week 1 | Week 2 | Week 3 |
|---|---|---|---|---|
| Monday | 9:00 | Restraint (1 h) | Restraint (1 h 30 min) | Restraint (1 h 50 min) |
| | 14:00 | Restraint (1 h) | Forced swimming (24°C, 30 min) | Forced swimming (15°C, 7 min) |
| | 18:00 | Food and water deprivation (15 h) | Less sawdust and water (15 h) | Water deprivation (15 h) |
| Tuesday | 9:00 | Restraint food (6 h 30 min) | Restraint (1 h 30 min) | Restraint (2 h) |
| | 14:00 | Restraint (1 h) | Restraint (1 h 30 min) | Restraint (2 h) |
| | 18:00 | Water deprivation (15 h) | Food and water deprivation (15 h) | Water deprivation (15 + 24 h) |
| Wednesday | 9:00 | Restraint (1 h 10 min) | Restraint (1 h 40 min) | Food deprivation (9 h) |
| | 14:00 | Damp sawdust (19 h) | Without sawdust and wet cage (19 h) | Restraint (2 h 10 min) |
| | 18:00 | | | |
| Thursday | 9:00 | Forced swimming (24°C, 30 min) | Restraint food (6 h 30 min) | Restraint (2 h 10 min) |
| | 14:00 | Restraint (1 h 10 min) | Restraint (1 h 40 min) | Tilted cage (40°, 24 h) |
| | 18:00 | Food deprivation (15 h) | Damp sawdust (15 h) + reversed light/dark cycle (24 h) | Damp sawdust (15 h) + reversed light/dark cycle (24 h) |
| Friday | 9:00 | Tilted cage (40°, 24 h) | Forced swim (24°C, 30 min) | Restraint (2 h 20 min) |
| | 14:00 | Restraint (1 h 20 min) | Restraint (1 h 50 min) | Restraint (2 h 20 min) |
| | 18:00 | Damp sawdust (15 h) + reversed light/dark cycle (24 h) | Tilted cage (40°, 15 h) + reversed light/dark cycle (24 h) | Tilted cage (40°, 15 h) |
| Saturday | All day | Reversed light/dark cycle (24 h) | Reversed light/dark cycle (24 h) | Reversed light/dark cycle (24 h) |
| Sunday | All day | Without sawdust + tilted cage (40°) + reversed light/dark cycle (24 h) | Less sawdust and water + tilted cage (40°) + reversed light/dark cycle (24 h) | Less sawdust and water + tilted cage (40°) + reversed light/dark cycle (24 h) |

antibody (1:10,000; Cat# ab181603, RRID:AB_2687666, Abcam). Primary antibodies were diluted in QuickBlock™ primary antibody dilution buffer (Cat#P0256, Beyotime Biotechnology) and reused at most three times. After the incubation, the membranes were washed and then incubated with HRP-conjugated secondary antibodies (goat anti-mouse IgG, Cat# GAM007, RRID:AB_2827834; goat anti-rabbit IgG, Cat# GAR007, RRID:AB_2827833, MultiSciences Biotech Co., Ltd, Hangzhou, China) for 2 h at room temperature. Secondary antibodies were diluted in TBS Tween and used once only. The proteins were revealed by enhanced chemiluminescence of the ECL detection kit (Cat#34577, Thermo Fisher Scientific). Quantitation of band density was conducted on analysis within the linear range and by a blinding approach. In statistical analysis, the protein level of the control group was always defined as 100%, and chemifluorescence was detected by ChemiDoc™ XRS+ Imaging system (Bio-Rad Laboratories, Hercules, CA, USA, RRID:SCR_008426). Each sample was repeated more than three times. The Immuno-related procedures used comply with the recommendations made by the *British Journal of Pharmacology* (Alexander et al., 2018).

## 2.8 | Co-immunoprecipitation

The co-immunoprecipitation (CO-IP) assay was performed as described previously (Zhou et al., 2010; Zhu et al., 2018). Briefly, the hippocampus of mice was homogenised in ice-cold lysis buffer A

(Cat# R0278; Sigma-Aldrich) for 30 min and then centrifuged at 20,000 $g$ for 15 min. The supernatant was pre-incubated for 1 h at 4°C with 0.02 ml of protein G-Sepharose beads (Cat# P4691; Sigma-Aldrich). It was then centrifuged to remove proteins that adhered non-specifically to the beads and to obtain the target supernatant for the following IP experiment. Protein G-Sepharose beads were incubated with an antibody (mouse antibody to nNOS, Cat# 610308, 5 μg; BD Transduction Laboratories) for 3–4 h. The antibody-conjugated protein G-Sepharose beads were incubated with the target supernatant overnight. The complexes were isolated using the centrifuge, washed four times with 0.05-M HEPES buffer pH 7.1 containing 0.15% Triton X-100 and 0.15-M NaCl. Bound proteins were eluted by heating the solution at 100°C in loading buffer. The analysis was conducted by immunoblotting.

## 2.9 | Immunocytochemistry and synaptic puncta

The details of the immunofluorescence assay for cultured neurons have been reported previously (Zhu et al., 2014). Neurons at 7 days in vitro were treated with 10-μM corticosterone in the presence of 0- or 10-μM ZLc-002 for 3 days. At 10 days in vitro, neurons were fixed and incubated with primary antibodies overnight at 4°C, followed by incubation with the secondary antibodies for 2 h at room temperature. The primary antibodies used were as follows: mouse anti-PSD-95 (1:300; Cat# ab2723, Abcam) and rabbit anti-synapsin (1:500;

Cat# AB1543P, Millipore Bioscience Research Reagents). The secondary antibodies used were goat anti-mouse Cy3 (1:200; Cat#115-165-003, RRID:AB_2338680, Jackson ImmunoResearch Laboratories) and goat anti-rabbit Alexa-647 (1:400; Cat# 111-605-003, RRID:AB_2338072, Jackson ImmunoResearch Laboratories). Images were captured using a confocal laser-scanning microscope (LSM700, Carl Zeiss, Oberkochen, Germany) at identical settings for each of the conditions and analysed with Imaris 7.2.3 software (Bitplane Scientific Software, Zurich, Switzerland, RRID: SCR_007370). Immunopositive puncta along dendrites and synapsin/PSD-95 double-positive puncta were counted. Only PSD-95 puncta with directly adjacent synapsin puncta were scored as colocalised synapsin/PSD-95 puncta.

## 2.10 | Analysis of neuronal dendritic complexity

Neurons at 4 days *in vitro* were treated with LV-GFP ($2 \times 10^8$ infectious units) for 24 h. At 10 days *in vitro*, neurons were fixed and incubated with a rabbit-anti-GFP primary antibody (1:800; Cat# ab290, RRID:AB_303395, Abcam) overnight at 4°C, followed by incubation with a goat anti-rabbit Alexa-Fluor 488 secondary antibody (1:400; Cat# 111-545-003, RRID:AB_2338046, Jackson ImmunoResearch Laboratories) for 2 h at room temperature. Images of GFP-labelled neurons were acquired using a confocal laser-scanning microscope (FV1000, Olympus, Tokyo, Japan) at identical settings for each of the conditions. Neurons were reconstructed using Imaris 7.2.3 software, and all analyses were performed using the ImageJ (National Institutes of Health, Bethesda, MD, USA, RRID:SCR_003070) Sholl Analysis Plugin. The length of each dendritic segment was determined by tracing the centre of the dendritic shaft. The number of dendritic intersections in concentric circles with various radii from the centroid of the soma was counted and plotted against the distance from the soma of the GFP^{+} neurons. The starting radius was 20 μm for neurons *in vitro*, and the ending radius was 200 μm for neurons *in vitro* from the centre. The interval between consecutive radii was 20 μm for neurons *in vitro*.

## 2.11 | Duolink Proximity Ligation Assay (PLA)

The proximal ligation assay was performed on cultured neurons with a Duolink *in s*itu detection kit as described previously (Almandoz-Gil et al., 2018). Primary neurons were fixed at 10 days *in vitro* with 4% PFA for 15 min at room temperature and 10 min at 4°C, followed with methanol for 1 min at −20°C, and then permeabilised with 0.1% Triton X-100 in PBS for 5 min. Cells were incubated with Duolink blocking solution for 30 min at 37°C, followed by incubation with monoclonal mouse nNOS (1:50; Cat# 610308, BD Transduction Laboratories), rabbit CAPON (1:200; Cat# ab190686, Abcam) and chicken β3-tubulin (1:500; Cat# 302306, RRID:AB_2620048; Synaptic Systems, Göttingen, Germany) primary antibodies diluted in Duolink Antibody diluent overnight at 4°C. The ligation assay was then conducted

following the instructions from the manufacturer (Cat# DUO92101, Sigma-Aldrich). β3-tubulin was detected using goat anti-chicken Alexa-488 (1:400; Cat# 103-545-155, RRID:AB_2337390; Jackson ImmunoResearch Laboratories). Images were captured using a confocal laser-scanning microscope (LSM700, Carl Zeiss) at identical settings for each of the conditions.

## 2.12 | Golgi-Cox staining

Golgi-Cox staining was performed as described previously (Zhu et al., 2014; Zhu et al., 2018). Fresh, non-perfused brains were used for Golgi-Cox staining with FD Rapid GolgiStain Kit (Cat# PK401; FD NeuroTechnologies, MD, USA) according to the user manual, and the brains were cut into 100-μm coronal sections using a vibratome (VT1000s; Leica). To calculate the spine density of Golgi-stained neurons in the dentate gyrus, a length of a dendrite was traced, the exact length of the dendritic segment was calculated and the number of spines along the dendritic segment was counted. Ten random neurons in each sample were measured, and the average was regarded as the final value for one sample.

## 2.13 | Data and statistical analysis

Data are presented as the mean ± SEM. The sample size, the number of independent values, was predetermined by our prior experience (Hu et al., 2012; Zhou et al., 2011; Zhu et al., 2014; Zhu et al., 2018). The control and test values (OD of target bands) in western blotting were first normalised to an internal standard (such as GAPDH) to reduce variance. Then all values (control and test) were normalised to the mean value of the experimental control group to set the Y-axis, so the control group value was 1. The units for these normalised data in the Y-axis were the fold of the control group's mean value. Statistical analysis was undertaken only for studies where each group size had at least five independent values. A one-way or two-way ANOVA was conducted using GraphPad Prism version 6.0 (La Jolla, CA, USA). The D'Agostino and Pearson omnibus normality test was carried out to assess the normality of data in the animal behavioural tests using GraphPad Prism version 6.0. Additionally, the Shapiro–Wilk normality test was conducted on normalised data from the biochemical tests using IBM SPSS version 20.0 (Armonk, NY, USA). If the group sizes were equal, the comparisons among multiple groups were performed with a one- or two-way ANOVA. If appropriate (only if F in ANOVA achieved the 'chosen' necessary level of statistical significance and there was no significant variance inhomogeneity), this was followed by Tukey's post hoc test. If the group sizes were unequal, the comparisons among multiple groups were performed with a two-way ANOVA. If appropriate, this was followed by Bonferroni's post hoc test. A P-value of <0.05 was considered statistically significant. Investigators were blinded to the treatment groups when assessing the outcomes. No values were excluded in the data analysis and presentation. The data and statistical analysis

comply with the recommendations of the *British Journal of Pharmacology* on experimental design and analysis in pharmacology (Curtis et al., 2018).

## 2.14 | Nomenclature of targets and ligands

Key protein targets and ligands in this article are hyperlinked to corresponding entries in http://www.guidetopharmacology.org, the common portal for data from the IUPHAR/BPS Guide to PHARMACOLOGY (Harding et al., 2018), and are permanently archived in the Concise Guide to PHARMACOLOGY 2019/20 (Alexander, Christopoulos, et al., 2019; Alexander, Cidlowski, et al., 2019).

## 3 | RESULTS

### 3.1 | nNOS–CAPON blockers attenuate chronic mild stress-induced anxiogenic behaviour

To identify the anxiolytic effects of nNOS–CAPON blockers in anxiety animal models, especially in the late phase of the chronic mild stress exposure, we used the chronic mild stress model in the adult male ICR mice to investigate whether treatment with ZLc-002, a small-molecule inhibitor of nNOS–CAPON interaction, can alleviate the anxiety behaviour induced by chronic mild stress. Adult mice were exposed to chronic mild stress for 4 weeks and treated with ZLc-002 (i.v., 40 mg·kg$^{-1}$·day$^{-1}$) for 7 days from day 21 to day 27 of chronic mild stress exposure. Their behaviour was examined 24 h after the last treatment. As expected, mice exposed to chronic mild stress displayed a typical anxiogenic phenotype, as indicated by the shortened time spent in open arms and the prolonged latency to feed in a novel environment compared with those of control mice (Figure 1b,d). Interestingly, ZLc-002 blocked the chronic mild stress-induced anxiogenic behaviours. In the elevated plus maze test, ZLc-002-treated mice exhibited a longer time spent in the open arms compared to vehicle-treated mice (Figure 1b). More importantly, we found that ZLc-002 treatment completely reversed the shortened time spent in the open arms induced by chronic mild stress exposure in mice but did not affect the number of entries to the open arms or total arms (Figure 1b,c). In the novelty-suppressed feeding test, ZLc-002 treatment significantly decreased the latency to feed in a novel environment in mice and reversed the chronic mild stress-induced latency increases to feed in a novel environment (Figure 1d). Neither ZLc-002 treatment nor chronic mild stress exposure affected the latency to feed or the amount of food consumption in the home cage (Figure 1d, e). In the open field test, ZLc-002 treatment or chronic mild stress exposure did not affect the locomotor activities of mice (Figure 1f,g), suggesting that the behavioural changes in the elevated plus maze and NSF tests cannot be explained by non-specific effects of treatments on activity levels. Altogether, these results indicate that ZLc-002 exerts anxiolytic effects.

To further determine the anxiolytic effect of nNOS–CAPON blockers, we examined the behaviour changes in chronic mild stress mice treated with Tat-CAPON12C, a peptide inhibitor of nNOS–CAPON association. Mutation of the penultimate alanine of CAPON-12C with aspartic acid renders it incapable of binding to nNOS (Jaffrey, Snowman, Eliasson, Cohen, & Snyder, 1998; Zhu et al., 2014). Therefore, we constructed a mutated peptide, Tat-CAPON-12C/A22D, as a control for Tat-CAPON-12C in our previous study. Adult male ICR mice were exposed to chronic mild stress for 4 weeks and treated with Tat-CAPON12C (i.v., 3 μmol·kg$^{-1}$·day$^{-1}$) or its control peptide (i.v., 3 μmol·kg$^{-1}$·day$^{-1}$) for 7 days from day 21 to day 27 of chronic mild stress exposure. Their behaviour was examined 24 h after the last treatment. Consistent with the previous reports, we found that Tat-CAPON-12C/A22D did not affect the chronic mild stress-induced anxiety-related behaviours in mice, compared to vehicle-treated chronic mild stress mice (Figure S2A–G). Similar to the behavioural modification actions of ZLc-002, we also showed that the intravenous administration of Tat-CAPON12C produced anxiolytic-like effects in the elevated plus maze and novelty-suppressed feeding tests (Figure 2b,d). More importantly, Tat-CAPON12C treatment reversed the chronic mild stress-induced reduction in time spent in the open arms in the elevated plus maze test and increase in the latency to feed in a novel environment in the novelty-suppressed feeding test (Figure 2b,d), indicating that Tat-CAPON12C prevented chronic mild stress-induced anxiogenic behaviours. Meanwhile, these treatments did not affect the number of entries in the total arms, the latency to feed in the home cages, the amount of home cage food consumption and locomotor activity in the novelty-suppressed feeding, elevated plus maze and open field tests, respectively (Figure 2c–g).

Therefore, these data indicate that the administration of nNOS–CAPON blockers, ZLc-002 or Tat-CAPON12C, for 7 days at the last week of chronic mild stress exposure can alleviate chronic mild stress-induced anxiety behaviours. This suggests that ZLc-002 and Tat-CAPON12C will have a therapeutic effect in chronic mild stress-induced anxiety disorders.

### 3.2 | nNOS–CAPON blockers reverse glucocorticoids-induced anxiogenic behaviours

Previously, our studies showed that chronic mild stress-induced glucocorticoid overproduction participates in the regulation of stress-related depressive and anxiety behaviours and using glucocorticoid treatment can mimic the behavioural effects of chronic mild stress (Zhou et al., 2011; Zhu et al., 2014; Zhu et al., 2018). Therefore, in this study, we also infused corticosterone (10 μM, 1 μl) daily into the hippocampus of adult male ICR mice for 28 days via pre-implanted cannula to model anxiety behaviours. To further confirm the therapeutic effects of nNOS–CAPON blockers on chronic stress-induced anxiety, we delivered ZLc-002 (10 μM, 1 μl, administrated 30 min after corticosterone) or Tat-CAPON12C (50 nM, 1 μl, administrated 30 min after corticosterone), into the hippocampus for 7 days from

day 21 to day 27 of corticosterone treatment. Behaviours were examined 24 h after the last treatment. Consistently, corticosterone-treated mice spent less time and fewer entries in the open arms in the elevated plus maze test, spent less time in the lit side in the light–dark test and had an increased latency to feed in a novel environment in the novelty-suppressed feeding test compared with vehicle-treated mice, displaying anxiogenic behaviours (Figures 3a–d and 4a,c,d). Our previous work showed that an intrahippocampal microinjection of ZLc-002 or Tat-CAPON12C produced anxiolytic-like effects in the elevated plus maze, novelty-suppressed feeding and light–dark tests (Zhu et al., 2014). Here, our results showed that ZLc-002 or Tat-CAPON12C significantly produced anxiolytic-like effects by intrahippocampal infusion for 7 consecutive days, compared to the vehicle or control peptide Tat-CAPON12C/A22D (Figure S3A–F). Notably, we found that ZLc-002 or Tat-CAPON12C infused into hippocampus abolished the corticosterone-induced shorter time spent in the open arms (Figures 3a and 4a), less time spent in the lit side (Figures 3c and 4c) and longer latency to feed in a novel environment (Figures 3d and 4d). However, the control peptide, Tat-CAPON12C/A22D, did not reverse the corticosterone-induced anxiety behaviours (Figure S4A–F). Corticosterone either alone or in combination with a ZLc-002 or Tat-CAPON12C microinjection did not affect the number of entries in the total arms, the latency to feed in home cages, the amount of home cage food consumption or locomotor activity in the elevated plus maze, novelty-suppressed feeding and open filed tests, respectively (Figures 3b,d–g and 4b,d–g). Chronic corticosterone microinjection did not alter the integrity of the infused hippocampus (Figure S1B).

Collectively, these results strongly indicate that ZLc-002 and Tat-CAPON12C have therapeutic effects in chronic stress-induced anxiety disorders.

## 3.3 | nNOS–CAPON blockers improve dendrites remodelling after chronic stress

Anxiety is related to neuroanatomical changes in the hippocampus (McLaughlin, Gomez, Baran, & Conrad, 2007; Mucha et al., 2011; Soetanto et al., 2010; Vyas, Mitra, Shankaranarayana Rao, & Chattarji, 2002; Warner-Schmidt & Duman, 2006). Accordingly, we evaluated whether nNOS–CAPON dissociation promoted structural remodelling in the hippocampal dentate gyrus of mice at a late stage of chronic mild stress exposure. Treatment of adult mice with ZLc-002 (i.v., 40 mg·kg$^{-1}$·day$^{-1}$) or Tat-CAPON12C (i.v., 3 μmol·kg$^{-1}$·day$^{-1}$)
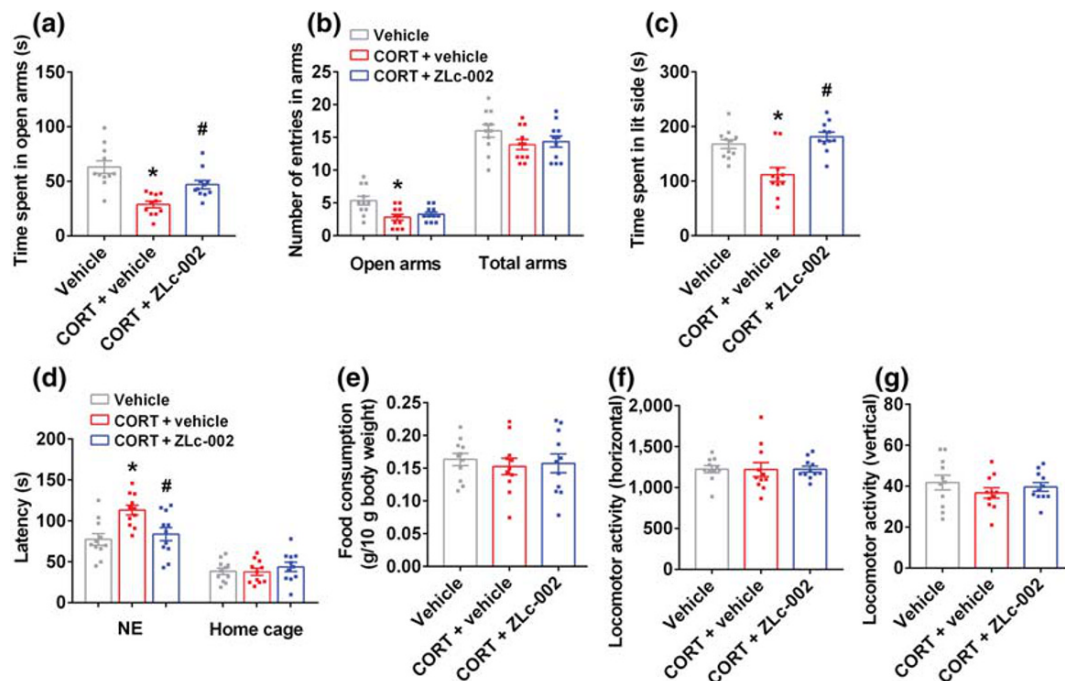


**FIGURE 3** ZLc-002 reverses the behavioural effects of glucocorticoids. (a–g) The adult male ICR mice were treated with 10-μM corticosterone (CORT) alone or in combination with 10-μM ZLc-002 by injection cannula. CORT or its vehicle was microinjected into the hippocampus for 28 consecutive days on day 4 after cannula implantation, ZLc-002 was intrahippocampal infusion on day 21 after CORT treatment for 7 consecutive days and the volume of each drug or its vehicle was 1.0 μl. (a) The time spent in open arms, and (b) number of entries in the arms in the elevated plus maze (EPM) test in adult mice. (c) Time spent in lit compartment of the light–dark box in adult mice. (d) The latency to feed in a novel environment and in the home cage, and (e) food consumption in the home cage in the novelty-suppressed feeding (NSF) test in adult mice. (f,g) The locomotor activity of mice in the open field test. Parameters for the locomotor activities were the number of square crossings (horizontal) and the time standing (vertical). Mean ± SEM, *n* = 11 mice in each group, [*]*P* < 0.05, compared with vehicle-treated group; [#]*P* < 0.05, compared with vehicle-treated and chronic CORT-infused group, one-way ANOVA followed by Tukey's post-test (a–f). NE, novel environment; total arms, open arms + enclosed arms
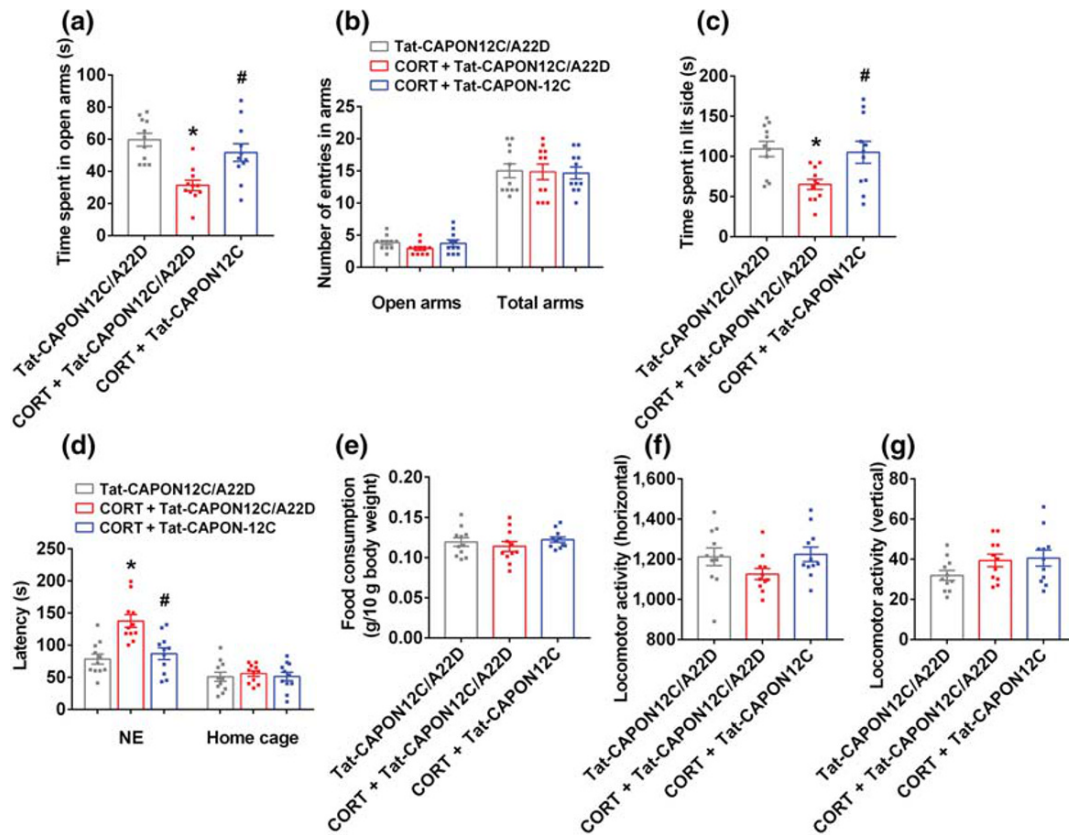
**FIGURE 4** Tat-CAPON12C reverses the behavioural effects of glucocorticoids. (a–g) The adult male ICR mice were treated with 10-μM corticosterone (CORT) alone or in combination with 50-nM Tat-CAPON12C or its control peptide Tat-CAPON12C/A22D by injection cannula. Corticosterone (CORT) or its vehicle was microinjected into the hippocampus for 28 consecutive days on day 4 after cannula implantation, Tat-CAPON12C or Tat-CAPON12C/A22D was intrahippocampal infusion on day 21 after CORT treatment for 7 consecutive days and the volume of each drug or its vehicle or control peptide was 1.0 μl. (a) The time spent in open arms, and (b) number of entries in the arms in the elevated plus maze (EPM) test in adult mice. (c) Time spent in lit compartment of the light–dark box in adult mice. (d) The latency to feed in a novel environment and in the home cage, and (e) food consumption in the home cage in the novelty-suppressed feeding (NSF) test in adult mice. (f,g) The locomotor activity of mice in the open field test. Parameters for the locomotor activities were the number of square crossings (horizontal) and the time standing (vertical). Mean ± SEM, $n$ = 11 mice in each group, $^*P < 0.05$, compared with Tat-CAPON12C/A22D-treated group; $^\#P < 0.05$, compared with Tat-CAPON12C/A22D-treated and chronic CORT-infused group, one-way ANOVA followed by Tukey's post-test (a–f). NE, novel environment; total arms, open arms + enclosed arms

increased dendritic spine density and rescued chronic mild stress-induced spine loss (Figure 5a–d). Moreover, ZLc-002 increased the dendritic length and branching of dendrites, the densities of synapsin and PSD-95 double-positive puncta in cultured hippocampal neurons (Figure 5e–j). Additionally, we found that ZLc-002 ameliorated the corticosterone-induced decrease in dendritic length, branching of dendrites, the densities of synapsin and PSD-95 double-positive puncta *in vitro* (Figure 5e–j). In agreement with previous studies, the results from the CO-IP assay demonstrated that ZLc-002 or Tat-CAPON12C treatment significantly decreased the amounts of nNOS–CAPON complex and reversed the chronic mild stress-induced nNOS–CAPON binding in the hippocampus of ICR mice (Figures 6a and 7a). Additionally, the *in situ* PLA showed that ZLc-002 (10 μM) significantly reduced the PLA signals (nNOS–CAPON interaction) in the soma of cultured neurons and reversed the enhancement of PLA signals induced by 10-μM corticosterone exposure for 72 h (Figure 6c). Consistent with morphological results, the western blot indicated that

Tat-CAPON12C and ZLc-002 increased the expression of synapsin and PSD-95, important proteins critical for synaptogenesis, in the hippocampus of mice (Figures 6b and 7b) and reversed the decreased level of synapsin and PSD-95 expression in hippocampus of chronic mild stress-exposed mice (Figures 6b and 7b). Additionally, ZLc-002 and Tat-CAPON12C also resulted in an increased expression of synapsin and PSD-95 and also reversed the corticosterone-induced synapsin and PSD-95 down-regulation in cultured hippocampal neurons (Figures 6d and 7c). These results suggest that nNOS–CAPON blockers increased synaptogenesis and improved dendritic remodelling.

To explore the molecular mechanism underlying the dendritic morphology changes after nNOS–CAPON blocking, we examined BDNF and p-CREB, two important signalling molecules related to synaptic structural plasticity. Both ZLc-002 and Tat-CAPON12C significantly increased the level of BDNF and p-CREB in the hippocampus of mice (Figures 6b and 7b). More importantly, ZLc-002 and Tat-
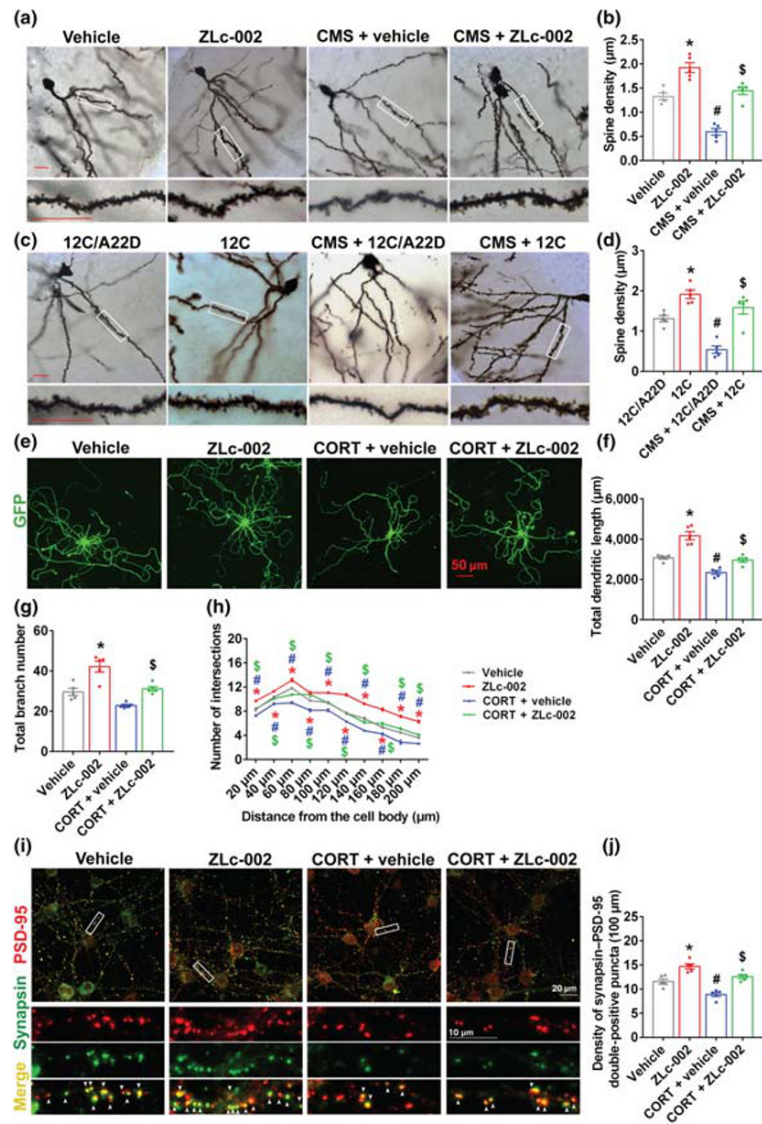
**FIGURE 5** nNOS–CAPON blockers rescue the chronic stress-induced synaptogenesis impairment. (a–d) The adult male ICR mice were treated with ZLc-002 (40 mg·kg$^{-1}$·day$^{-1}$) or Tat-CAPON12C (3 μmol·kg$^{-1}$·day$^{-1}$) or vehicle or control peptide by intravenous administration for 7 consecutive days on 21 days after CMS exposure. (a,b) Dissociating nNOS–CAPON by ZLc-002 rescues the CMS-induced spine loss of dentate gyrus (DG) granule cells. Representative images with Golgi-Cox staining (a) and bar graph (b) showing dendrite spine density of granular cells in the hippocampal DG of mice administered with ZLc-002 and exposed to CMS ($n$ = 5 mice in each group, 10 neurons per sample). Scale bar, 20 μm. $^*P < 0.05$, compared with vehicle-treated group; $^\#P < 0.05$, compared with vehicle-treated non-CMS group; $^\$P < 0.05$, compared with vehicle-treated CMS group. (c,d) Dissociating nNOS–CAPON by Tat-CAPON12C rescues the CMS-induced spine loss of DG granule cells. Representative images with Golgi-Cox staining (c) and bar graph (d) showing dendrite spine density of granular cells in the hippocampal DG of mice administered with Tat-CAPON12C and exposed to CMS ($n$ = 5 mice in each group, 10 neurons per sample). Scale bar, 20 μm. $^*P < 0.05$, compared with 12C/A22D-treated group; $^\#P < 0.05$, compared with 12C/A22D-treated non-CMS group; $^\$P < 0.05$, compared with 12C/A22D-treated CMS group. (e–h) Dendrites growth of neurons treated with 10-μM CORT alone or in combination with 10-μM ZLc-002 or vehicle for 72 h. (e) Representative images of GFP$^+$ neurons exposure to corticosterone (CORT) with ZLc-002 or vehicle. Scale bar, 50 μm. (f) Bar graph showing total dendritic length of neurons treated with CORT alone or in combination with ZLc-002 or vehicle ($n$ = 5 in each group, from five independent experiments, 10 neurons per sample). (g) Bar graph showing total branch number of neurons treated with ZLc-002 or vehicle after CORT exposure ($n$ = 5 in each group, from five independent experiments, 10 neurons per sample). (h) Sholl analysis of dendritic complexity of neurons treated with ZLc-002 or vehicle after CORT exposure ($n$ = 5 in each group, from five independent experiments, 10 neurons per sample). (i) Representative images of neurons stained for synapsin/PSD-95 with or without 10-μM ZLc-002 treatment after 10-μM CORT exposure (upper) and representative images of synapsin-positive puncta, PSD-95-positive puncta and synapsin/PSD-95 double-positive puncta along dendrites of neurons selected from boxed areas (lower). These images were selected from boxed areas. Arrows indicate synapsin/PSD-95 double-positive puncta. Scale bar, 10 or 20 μm. (j) Bar graph showing densities of synapsin/PSD-95 double-positive puncta along dendrites of neurons treated by CORT in combination with ZLc-002 or vehicle for 72 h ($n$ = 5 in each group, from five independent experiments, 12 neurons per sample). For (f)–(h) and (j), $^*P < 0.05$: ZLc-002 versus vehicle; $^\#P < 0.05$: CORT + vehicle versus vehicle; $^\$P < 0.05$: CORT + ZLc-002 versus CORT + vehicle. Mean ± SEM, two-way ANOVA followed by Tukey's post-test. 12C/A22D, Tat-CAPON12C/A22D; 12C, Tat-CAPON12C
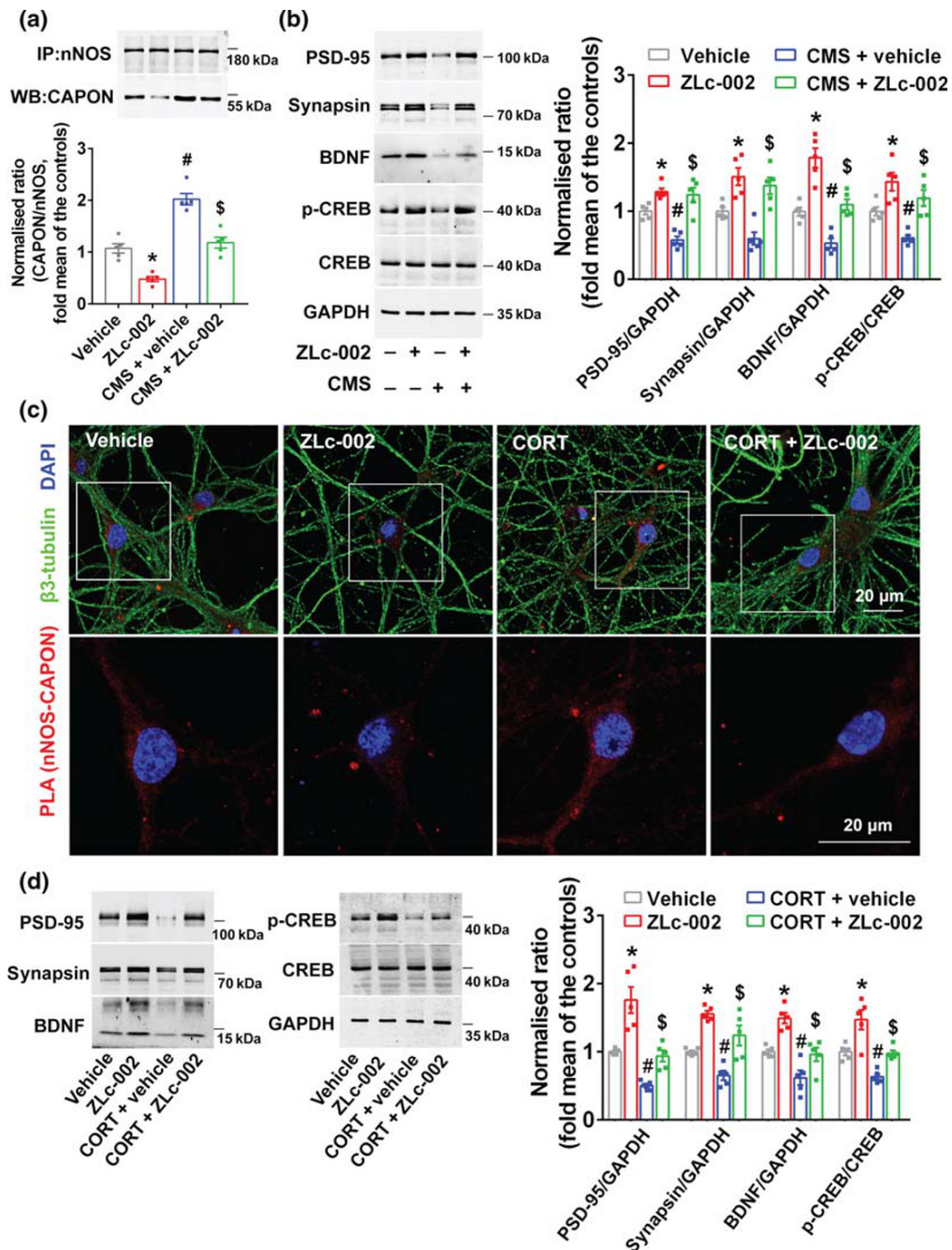
**FIGURE 6** CREB–BDNF signalling is involved in the effects of ZLc-002 on synaptogenesis impairment induced by chronic stress. (a,b) The adult male ICR mice were treated with ZLc-002 (40 mg·kg$^{-1}$·day$^{-1}$) or its vehicle by intravenous administration for 7 consecutive days on 21 days after CMS exposure. (a) ZLc-002 treatment reduced the amounts of nNOS–CAPON complex (presented as the ratio of CAPON to nNOS) in the hippocampus of mice exposed to CMS for 28 days ($n = 5$ mice in each group). (b) Representative immunoblots (left) and bar graph (right) showing PSD-95, synapsin, BDNF, p-CREB and CREB in the hippocampus of mice treated with ZLc-002 and exposed to CMS ($n = 5$ mice in each group). (c,d) The cultured neurons treated with 10-μM corticosterone (CORT) alone or in combination with 10-μM ZLc-002 or their vehicle for 72 h. (c) Representative confocal images of in situ proximity ligation assay (PLA) between nNOS and CAPON (red) in primary neurons. Maximum intensity projections of a confocal z-stack including a whole cell were performed to observe the maximum amount of PLA puncta. The neurons were counter-stained with β3-tubulin (green) and DAPI (blue). Scale bar: 20 μm. (d) Representative immunoblots (left) and bar graph (right) showing PSD-95, synapsin, BDNF and p-CREB in the cultured hippocampal neurons treated with ZLc-002 and exposed to CORT ($n = 5$ in each group, from five independent experiments). For (a) and (b), *$P < 0.05$, compared with vehicle-treated group; #$P < 0.05$, compared with vehicle-treated non-CMS group; $P < 0.05$, compared with vehicle-treated CMS group; for (d), *$P < 0.05$, compared with vehicle-treated group; #$P < 0.05$, compared with vehicle-treated group; $P < 0.05$, compared with vehicle-treated CORT-incubated group. Mean ± SEM, two-way ANOVA followed by Tukey's post-test
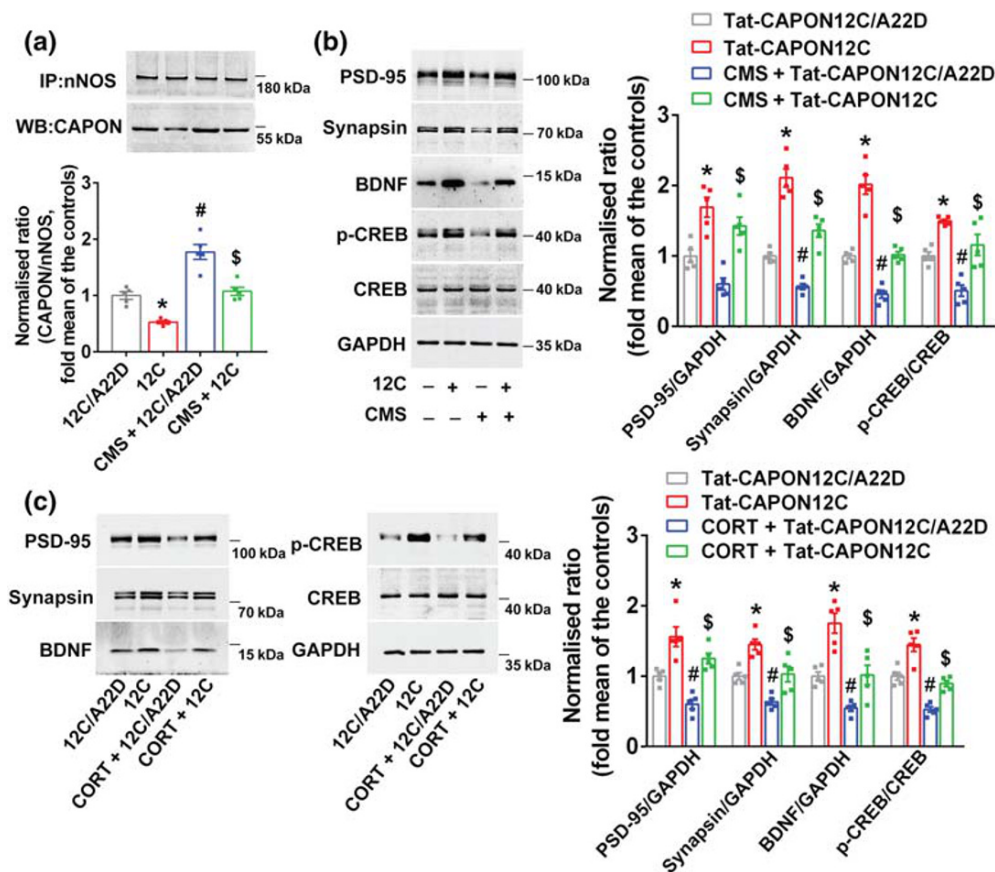
**FIGURE 7** CREB–BDNF signalling is involved in the effects of Tat-CAPON12C on synaptogenesis impairment induced by chronic stress. (a,b) The adult male ICR mice were treated with Tat-CAPON12C (3 $\mu$mol·kg$^{-1}$·day$^{-1}$) or its control peptide Tat-CAPON12C/A22D by intravenous administration for 7 consecutive days on 21 days after CMS exposure. (a) Tat-CAPON12C treatment reduced the amounts of nNOS–CAPON complex (presented as the ratio of CAPON to nNOS) in the hippocampus of mice exposed to CMS for 28 days ($n$ = 5 mice in each group). (b) Representative immunoblots (left) and bar graph (right) showing PSD-95, synapsin, BDNF and p-CREB in the hippocampus of mice treated with Tat-CAPON12C and exposed to CMS ($n$ = 5 mice in each group). (c) The cultured neurons treated with 10-$\mu$M corticosterone (CORT) alone or in combination with 50-nM Tat-CAPON12C or its control peptide for 72 h. Representative immunoblots (left) and bar graph (right) showing PSD-95, synapsin, BDNF and p-CREB in the cultured hippocampal neurons treated with Tat-CAPON12C and exposed to CORT ($n$ = 5 in each group, from five independent experiments). For (a) and (b), $^*P$ < 0.05, compared with 12C/A22D-treated group; $^\#P$ < 0.05, compared with 12C/A22D-treated non-CMS group; $^\$P$ < 0.05, compared with 12C/A22D-treated CMS group; for (c), $^*P$ < 0.05, compared with 12C/A22D-treated group; $^\#P$ < 0.05, compared with 12C/A22D-treated group; $^\$P$ < 0.05, compared with 12C/A22D-treated CORT-incubated group. Mean ± SEM, two-way ANOVA followed by Tukey's post-test. 12C/A22D, Tat-CAPON12C/A22D; 12C, Tat-CAPON12C

CAPON12C abolished the chronic mild stress-induced BDNF and p-CREB down-regulation (Figures 6b and 7b). Additionally, we found that ZLc-002 and Tat-CAPON12C also increased levels of BDNF and p-CREB and reversed the corticosterone-triggered reduction of BDNF and p-CREB in cultured neurons (Figures 6d and 7c). These effects on the expression of PSD-95, synapsin, BDNF and p-CREB were not present in nNOS-knockout mice (Figure S5A,B).

In conclusion, blocking nNOS–CAPON interaction can reverse changes in dendritic morphology and in the CREB–BDNF pathway induced by chronic stress.

## 4 | DISCUSSION

Anxiety disorders are a highly prevalent and leading cause of disability that result in significant financial and emotional burdens for people

worldwide (Crocq, 2017; Hawgood & De Leo, 2008; Sareen et al., 2005). Currently, SSRIs and BZDs are widely prescribed anxiolytics. Due to the side effects of BZDs and the delayed onset of action of SSRIs, there are few clinically safe and rapidly efficacious anxiolytics. We previously found that nNOS–CAPON coupling contributes to the regulation of anxiety behaviours and dissociation of nNOS with CAPON produces anxiolytic-like effects under physiological conditions. Here, we have demonstrated that nNOS–CAPON blockers have potent anxiolytic effects in two chronic stress-induced anxiety animal models, implicating nNOS–CAPON inhibitors for the treatment of anxiety disorders. Also, stroke, neuropathic pain and early-stage Alzheimer's disease are associated with the co-morbid anxiety (Bierman, Comijs, Jonker, Scheltens, & Beekman, 2009; Campbell Burton et al., 2013; Knapp et al., 2017; Kwak, Yang, & Koo, 2017; Nicholson & Verma, 2004). Reportedly, nNOS–CAPON association mediates amyloid-$\beta$-induced neurotoxicity (Zhang et al., 2018),

ischaemia-induced impairment of structural plasticity (Ni et al., 2018) and inflammatory nociception and chemotherapy-induced neuropathic pain (Lee, Carey, et al., 2018; Lee, Li, et al., 2018). We previously reported that dissociation of nNOS with CAPON by ZLc-002 produces rapid onset of anxiolytic-like effect (Zhu et al., 2014). Taken together, nNOS–CAPON inhibitors may serve as potential and promising anxiolytics. The inhibitors could have wider implications, not only for treating primary anxiety disorders but also for the co-morbid of anxiety associated with neuropathological diseases including stroke, neuropathic pain and Alzheimer's disease.

Previously, we reported that intrahippocampal injection of Tat-CAPON12C competes with CAPON for the C-terminal ligand-binding site on PDZ domain of nNOS, destabilises nNOS–CAPON interactions in the hippocampus and produces anxiolytic-like effects (Zhu et al., 2014). Here, we demonstrated that the peptide inhibitor Tat-CAPON12C, but not the putative inactive peptide Tat-CAPON12C/A22D, disrupted the binding between nNOS and CAPON in vivo. More importantly, we found that intravenous administration of Tat-CAPON12C, but not Tat-CAPON12C/A22D, at a late stage of chronic mild stress exposure reversed chronic stress-induced nNOS–CAPON binding and anxiogenic behaviours. In the current study, we also verified that the small-molecule inhibitor ZLc-002 dissociated nNOS from CAPON and reversed chronic mild stress exposure-induced alterations in the hippocampal nNOS–CAPON binding in adult mice as shown by a CO-IP assay. Furthermore, we evaluated the ability of ZLc-002 to disrupt nNOS–CAPON interactions through a Duolink PLA and found that ZLc-002 significantly decreased the signal of nNOS–CAPON proximity ligation and prevented chronic corticosterone exposure-induced nNOS–CAPON coupling in the cultured hippocampal neurons. Although our previous research found that ZLc-002 is a small-molecule compound that possesses anxiolytic-like effects with rapid onset of action and with little side effects under physiological conditions, its therapeutic effects on animal anxiety models are worthy of further study. In the current study, we further evaluated the anxiolytic effects of nNOS–CAPON blockers on chronic stress-induced animal models. Unlike the previous study, both ZLc-002 and Tat-CAPON12C were administered intravenously during the last week of chronic mild stress exposure. The results showed that treatment with ZLc-002 or Tat-CAPON12C at a late stage of chronic mild stress exposure abolished the behavioural effects of chronic mild stress in animal anxiety models. Additionally, we also examined the anxiolytic effects of ZLc-002 and Tat-CAPON12C in chronic corticosterone-exposed animal models. Similar to the results in the chronic mild stress-induced anxiety in animals, we also found that ZLc-002 and Tat-CAPON12C reversed the chronic corticosterone-induced anxiety behaviours. The findings of our current study indicate that these blockers may be beneficial for treating anxiety disorders.

Numerous reports have indicated that anxiety disorders are associated with neuroanatomical changes in the hippocampus and that chronic stress, one of the leading causes of anxiety disorders, significantly impairs hippocampal synaptic plasticity (McLaughlin et al., 2007; Mucha et al., 2011; Soetanto et al., 2010; Vyas et al., 2002; Warner-Schmidt & Duman, 2006). We have examined the

therapeutic effects of nNOS–CAPON disruptors, but the underlying neural mechanism is still unclear. Our current study found that treatment of Tat-CAPON12C or ZLc-002 intravenously at the late stage of chronic mild stress exposure rescued chronic stress-induced dendritic morphology alterations in vivo. Moreover, ZLc-002 reversed the reduction of dendritic branching induced by chronic corticosterone exposure in cultured neurons. PSD-95 and synapsin are two important proteins, specifically located at postsynaptic and presynaptic sites, respectively, that have been implicated in synaptogenesis (Cline, 2005; Kao et al., 1998). The density of PSD-95 and synapsin partially reflects the efficacy of synaptic connections. Our present work has shown that ZLc-002 increased the level of PSD-95 and synapsin and also reversed the chronic mild stress or chronic corticosterone exposure-induced reduction in the expression of PSD-95 and synapsin in vivo and in vitro. Furthermore, ZLc-002 reversed the chronic corticosterone exposure-induced reduction in the densities of synapsin and PSD-95-positive puncta. These results suggest that nNOS–CAPON inhibitors possess anxiolytic effects via promoting synaptogenesis.

nNOS is the main NOS in the hippocampus, differing from its isoenzymes inducible NOS (iNOS) and endothelial NOS (eNOS) in its PDZ domain, which can interact with many adapter proteins and thus affect its physiological functions (Zhou & Zhu, 2009). An increasing number of reports indicate that nNOS is involved in many pathological conditions, such as anxiety, depression and Alzheimer's disease (Hu et al., 2012; Zhang et al., 2010; Zhou et al., 2007; Zhou et al., 2011; Zhou, Zhu, Nemes, & Zhu, 2018; Zhu et al., 2014; Zhu et al., 2018). Among the adapter proteins of nNOS, other researchers and ourselves have found that CAPON is related to emotional diseases (Brzustowicz, 2008; Delorme et al., 2010; Lawford et al., 2013; Xu et al., 2005; Zhu et al., 2014; Zhu et al., 2018). It has a PDZ domain at the C-terminus, which can bind to nNOS, and a phosphotyrosine binding domain at the N-terminus, which can bind to Dexras1, to form an nNOS–CAPON–Dexras1 ternary complex adjacent to the NMDA receptor (Cheah et al., 2006; Fang et al., 2000; Jaffrey et al., 1998). The juxtaposition of nNOS and Dexras1 can increase the S-nitrosylation of NO on Dexras1, convert the Dexras1-GDP into the active state of Dexras1-GTP and activate Dexras1 via **NMDA receptor**-gated calcium (Cheah et al., 2006; Fang et al., 2000). Dexras1, also known as AGS1 or RASD1, belongs to one of the small G-protein ras families and regulates the downstream of the G protein signalling, such as ERK, adenylate cyclase and the NMDA receptor–NO-mediated signalling pathway (Fang et al., 2000; Graham, Qiao, & Dorin, 2004; Nguyen & Watts, 2005). Previously, we found that augment of nNOS–CAPON coupling by over-expression of full-length CAPON significantly increases the level of nitrosylation of Dexras1 and decreases the level of phosphorylation of ERK. Contrastingly, the dissociation of nNOS from CAPON by ZLc-002 or by the over-expression of CAPON-125C decreases the level of nitrosylated Dexras1 and increases the level of p-ERK (Zhu et al., 2014). These findings implicate that Dexras1–ERK signalling is involved in the regulation of anxiety-related behaviours of nNOS–CAPON interactions under physiological conditions. It is generally believed that ERK

pathway activation triggers CREB phosphorylation and then increases BDNF expression by promoting the BDNF promoters (Karpova et al., 2013; Wang & Mao, 2019; Xing, Ginty, & Greenberg, 1996). The ERK–CREB–BDNF signalling pathway is closely related to synaptic plasticity and promoting activation of this pathway might slow the development of affective disorders, such as anxiety disorders (Duman & Voleti, 2012; Giachello et al., 2010; Krishnan & Nestler, 2008; Martinowich, Manji, & Lu, 2007; Song, Martinowich, & Lee, 2017; Wang & Mao, 2019). Our present work has shown that ZLc-002 and Tat-CAPON12C increase the level of BDNF and p-CREB in vivo and *in vitro*. More importantly, we found that treatment of Tat-CAPON12C or ZLc-002 intravenously at the late stage of chronic mild stress exposure reversed chronic stress-induced BDNF and p-CREB down-regulation in vivo and reversed the chronic corticosterone incubation-triggered BDNF and p-CREB reduction *in vitro*. The previous studies showed that NO donor DETA/NONOate significantly decreased p-CREB (Luo et al., 2010), whereas p-CREB level in the hippocampus of nNOS inhibitor (7-NI)-treated mice and nNOS knockout mice was significantly enhanced (Luo et al., 2007). There are studies that reported that inhibition of nNOS-derived NO enhanced the expression of BDNF mRNA and protein *in vitro* and increased the BDNF content in the neocortex (Xiong et al., 1999). Moreover, inhibition of nNOS increased BDNF secretion, whereas exogenous NO administration decreased BDNF secretion (Canossa, Giordano, Cappello, Guarnieri, & Ferri, 2002). Consistent with these findings, our present work has shown that nNOS knockout increases the level of p-CREB and BDNF. Therefore, the anxiolytic effects of nNOS–CAPON blockers may come from the recovery of the down-regulation of CREB–BDNF signalling induced by chronic stress.

In summary, we report that dissociation of nNOS–CAPON by a small-molecule ZLc-002 or peptide inhibitor Tat-CAPON12C at the late stage of chronic stress exposure reverses the behavioural effects, dendritic outgrowth and synaptogenesis impairments in chronic stress-induced anxiety animal models. nNOS and its adapter protein CAPON are present not only in excitatory neurons but also in inhibitory neurons. Therefore, more studies are needed to determine the influence of nNOS–CAPON disruptors on the dendritic morphology and synapse formation of inhibitory neurons. The observations of stress-induced changes in glutamatergic and GABAergic neurotransmission imply that disturbances of excitatory and inhibitory neurotransmission are implicated in stress-related anxiety disorders (Brambilla, Perez, Barale, Schettini, & Soares, 2003; Farb & Ratner, 2014; Sanacora, Zarate, Krystal, & Manji, 2008). Therefore, further investigations need to be conducted on whether and how nNOS–CAPON blockers can produce anxiolytic effects by modifying the hippocampal excitatory–inhibitory equilibrium.

## AUTHOR CONTRIBUTIONS

D.Y.Z. conceived the project; L.J.Z. wrote the manuscript; L.J.Z., H.J.S., L.C., C.C.Z. and M.S. performed the experiments and analysed the data; and N.L. assisted in some experiments and the data analyses. All authors approved the final version of the manuscript. We thank Y. Tang for her advice in writing the article.

## CONFLICT OF INTEREST

The authors declare no conflicts of interest.

## DECLARATION OF TRANSPARENCY AND SCIENTIFIC RIGOUR

This Declaration acknowledges that this paper adheres to the principles for transparent reporting and scientific rigour of preclinical research as stated in the *BJP* guidelines for Design & Analysis, Immunoblotting and Immunochemistry, and Animal Experimentation, and as recommended by funding agencies, publishers and other organisations engaged with supporting research.

## REFERENCES

Alexander, S. P. H., Christopoulos, A., Davenport, A. P., Kelly, E., Mathie, A., Alistair, P., & CGTP Collaborators (2019). THE CONCISE GUIDE TO PHARMACOLOGY 2019/20: G protein-coupled receptors. *British Journal of Pharmacology*, *176*, S21–S141. https://doi.org/10.1111/bph.14748

Alexander, S. P. H., Cidlowski, J. A., Kelly, E., Mathie, A., Peters, J. A., & Veale, E. L. (2019). THE CONCISE GUIDE TO PHARMACOLOGY 2019/20: Nuclear hormone receptors. *British Journal of Pharmacology*, *176*, S229–S246. https://doi.org/10.1111/bph.14750

Alexander, S. P. H., Roberts, R. E., Broughton, B. R. S., Sobey, C. G., George, C. H., Stanford, S. C., … Ahluwalia, A. (2018). Goals and practicalities of immunoblotting and immunohistochemistry: A guide for submission to the *British Journal of Pharmacology*. *British Journal of Pharmacology*, *175*(3), 407–411. https://doi.org/10.1111/bph.14112

Almandoz-Gil, L., Persson, E., Lindström, V., Ingelsson, M., Erlandsson, A., & Bergström, J. (2018). In situ proximity ligation assay reveals co-localization of alpha-synuclein and SNARE proteins in murine primary neurons. *Frontiers in Neurology*, *9*, 180. https://doi.org/10.3389/fneur.2018.00180

Bannerman, D. M., Sprengel, R., Sanderson, D. J., McHugh, S. B., Rawlins, J. N., Monyer, H., & Seeburg, P. H. (2014). Hippocampal synaptic plasticity, spatial memory and anxiety. *Nature Reviews. Neuroscience*, *15*(3), 181–192. https://doi.org/10.1038/nrn3677

Bierman, E. J., Comijs, H. C., Jonker, C., Scheltens, P., & Beekman, A. T. (2009). The effect of anxiety and depression on decline of memory function in Alzheimer's disease. *International Psychogeriatrics*, *21*, 1142–1147. https://doi.org/10.1017/S1041610209990512

Brambilla, P., Perez, J., Barale, F., Schettini, G., & Soares, J. C. (2003). GABAergic dysfunction in mood disorders. *Molecular Psychiatry*, *8*(8), 721–737. https://doi.org/10.1038/sj.mp.4001362

Brzustowicz, L. M. (2008). NOS1AP in schizophrenia. *Current Psychiatry Reports*, *10*(2), 158–163. https://doi.org/10.1007/s11920-008-0027-0

Cai, C. Y., Wu, H. Y., Luo, C. X., Zhu, D. Y., Zhang, Y., Zhou, Q. G., & Zhang, J. (2019). Extracellular regulated protein kinase is critical for the role of 5-HT1a receptor in modulating nNOS expression and anxiety-related behaviors. *Behavioural Brain Research*, **357-358**, 88–97. https://doi.org/10.1016/j.bbr.2017.12.017

Campbell Burton, C. A., Murray, J., Holmes, J., Astin, F., Greenwood, D., & Knapp, P. (2013). Frequency of anxiety after stroke: A systematic review and meta-analysis of observational studies. *International Journal of Stroke*, *8*(7), 545–559. https://doi.org/10.1111/j.1747-4949.2012.00906.x

Canossa, M., Giordano, E., Cappello, S., Guarnieri, C., & Ferri, S. (2002). Nitric oxide down-regulates brain-derived neurotrophic factor secretion in cultured hippocampalneurons. *Proceedings of the National Academy of Sciences of the United States of America*, *99*(5), 3282–3287. https://doi.org/10.1073/pnas.042504299

Cheah, J. H., Kim, S. F., Hester, L. D., Clancy, K. W., Patterson, S. E. 3rd, Papadopoulos, V., & Snyder, S. H. (2006). NMDA receptor-nitric oxide transmission mediates neuronal iron homeostasis via the GTPase Dexras1. *Neuron*, *51*, 431–440. https://doi.org/10.1016/j.neuron.2006.07.011

Cline, H. (2005). Synaptogenesis: A balancing act between excitation and inhibition. *Current Biology*, *15*(6), R203–R205. https://doi.org/10.1016/j.cub.2005.03.010

Crocq, M. A. (2017). The history of generalized anxiety disorder as a diagnostic category. *Dialogues in Clinical Neuroscience*, *19*(2), 107–116.

Cryan, J. F., & Sweeney, F. F. (2011). The age of anxiety: Role of animal models of anxiolytic action in drug discovery. *British Journal of Pharmacology*, *164*(4), 1129–1161. https://doi.org/10.1111/j.1476-5381.2011.01362.x

Curtis, M. J., Alexander, S., Cirino, G., Docherty, J. R., George, C. H., Giembycz, M. A., … Ahluwalia, A. (2018). Experimental design and analysis and their reporting II: Updated and simplified guidance for authors and peer reviewers. *British Journal of Pharmacology*, *175*(7), 987–993. https://doi.org/10.1111/bph.14153

Delorme, R., Betancur, C., Scheid, I., Anckarsäter, H., Chaste, P., Jamain, S., … Mouren, M. C. (2010). Mutation screening of NOS1AP gene in a large sample of psychiatric patients and controls. *BMC Medical Genetics*, *11*, 108.

Ducottet, C., Griebel, G., & Belzung, C. (2003). Effects of the selective nonpeptide corticotropin-releasing factor receptor 1 antagonistantalarmin in the chronic mild stress model of depression in mice. *Progress in Neuro-Psychopharmacology & Biological Psychiatry*, *27*(4), 625–631. https://doi.org/10.1016/S0278-5846(03)00051-4

Duman, R. S., & Voleti, B. (2012). Signaling pathways underlying the pathophysiology and treatment of depression: Novel mechanisms for rapid-acting agents. *Trends in Neurosciences*, *35*(1), 47–56. https://doi.org/10.1016/j.tins.2011.11.004

Fang, M., Jaffrey, S. R., Sawa, A., Ye, K., Luo, X., & Snyder, S. H. (2000). Dexras1: A G protein specifically coupled to neuronal nitric oxide synthase via CAPON. *Neuron*, *28*, 183–193. https://doi.org/10.1016/s0896-6273(00)00095-7

Farb, D. H., & Ratner, M. H. (2014). Targeting the modulation of neural circuitry for the treatment of anxiety disorders. *Pharmacological Reviews*, *66*(4), 1002–1032.

Giachello, C. N., Fiumara, F., Giacomini, C., Corradi, A., Milanese, C., Ghirardi, M., … Montarolo, P. G. (2010). MAPK/Erk-dependent phosphorylation of synapsin mediates formation of functional synapses and short-term homosynaptic plasticity. *Journal of Cell Science*, *123*(Pt 6), 881–893. https://doi.org/10.1242/jcs.056846

Graham, T. E., Qiao, Z., & Dorin, R. I. (2004). Dexras1 inhibits adenylyl cyclase. *Biochemical and Biophysical Research Communications*, *316*, 307–312. https://doi.org/10.1016/j.bbrc.2004.02.049

Harding, S. D., Sharman, J. L., Faccenda, E., Southan, C., Pawson, A. J., & Ireland, S. (2018). The IUPHAR/BPS guide to pharmacology in 2018: Updates and expansion to encompass the new guide to immunopharmacology. *Nucleic Acids Research*, *46*, D1091–D1091. https://doi.org/10.1093/nar/gkx1121

Hawgood, J., & De Leo, D. (2008). Anxiety disorders and suicidal behaviour: An update. *Current Opinion in Psychiatry*, *21*, 51–64. https://doi.org/10.1097/YCO.0b013e3282f2309d

Hu, Y., Wu, D. L., Luo, C. X., Zhu, L. J., Zhang, J., Wu, H. Y., & Zhu, D. Y. (2012). Hippocampal nitric oxide contributes to sex difference in affective behaviors. *Proceedings of the National Academy of Sciences of the United States of America*, *109*(35), 14224–14229.

Jaffrey, S. R., Snowman, A. M., Eliasson, M. J., Cohen, N. A., & Snyder, S. H. (1998). CAPON: A protein associated with neuronal nitric oxide synthase that regulates its interactions with PSD-95. *Neuron*, *20*, 115–124. https://doi.org/10.1016/s0896-6273(00)80439-0

Kao, H. T., Porton, B., Czernik, A. J., Feng, J., Yiu, G., Häring, M., … Greengard, P. (1998). A third member of the synapsin gene family. *Proceedings of the National Academy of Sciences of the United States of America*, *95*(8), 4667–4672.

Karpova, A., Mikhaylova, M., Bera, S., Bär, J., Reddy, P. P., Behnisch, T., … Kreutz, M. R. (2013). Encoding and transducing the synaptic or extrasynaptic origin of NMDA receptor signals to the nucleus. *Cell*, *152*(5), 1119–1133. https://doi.org/10.1016/j.cell.2013.02.002

Kilkenny, C., Browne, W., Cuthill, I. C., Emerson, M., & Altman, D. G. (2010). Animal research: Reporting in vivo experiments: The ARRIVE guidelines. *British Journal of Pharmacology*, *160*, 1577–1579. https://doi.org/10.1111/j.1476-5381.2010.00872.x

Knapp, P., Burton, C. A. C., Holmes, J., Murray, J., Gillespie, D., Lightbody, C. E., & Watkins, C. L. (2017). Interventions for treating anxiety after stroke. *Cochrane Database of Systematic Reviews*, *5*, CD008860.

Krishnan, V., & Nestler, E. J. (2008). The molecular neurobiology of depression. *Nature*, *16*, *455*(7215), 894–902. https://doi.org/10.1038/nature07455

Kwak, Y. T., Yang, Y., & Koo, M. S. (2017). Anxiety in dementia. *Dement Neurocogn Disord*, *16*(2), 33–39. https://doi.org/10.12779/dnd.2017.16.2.33

Lawford, B. R., Morris, C. P., Swagell, C. D., Hughes, I. P., Young, R. M., & Voisey, J. (2013). NOS1AP is associated with increased severity of PTSD and depression in untreated combat veterans. *Journal of Affective Disorders*, *147*, 87–93. https://doi.org/10.1016/j.jad.2012.10.013

Lee, W. H., Carey, L. M., Li, L. L., Xu, Z., Lai, Y. Y., Courtney, M. J., & Hohmann, A. G. (2018). ZLc002, a putative small-molecule inhibitor of nNOS interaction with NOS1AP, suppresses inflammatory nociception and chemotherapy-induced neuropathic pain and synergizes with paclitaxel to reduce tumor cell viability. *Molecular Pain*, *14*, 1–17.

Lee, W. H., Li, L. L., Chawla, A., Hudmon, A., Lai, Y. Y., Courtney, M. J., & Hohmann, A. G. (2018). Disruption of nNOS-NOS1AP protein-protein interactions suppresses neuropathic pain in mice. *Pain*, *159*(5), 849–863. https://doi.org/10.1097/j.pain.0000000000001152

Luo, C. X., Jin, X., Cao, C. C., Zhu, M. M., Wang, B., Chang, L., … Zhu, D. Y. (2010). Bidirectional regulation of neurogenesis by neuronal nitric oxide synthase derived from neurons and neural stem cells. *Stem Cells*, *28*(11), 2041–2052. https://doi.org/10.1002/stem.522

Luo, C. X., Zhu, X. J., Zhou, Q. G., Wang, B., Wang, W., Cai, H. H., … Zhu, D. Y. (2007). Reduced neuronal nitric oxide synthase is involved in ischemia-induced hippocampal neurogenesis by up-regulating inducible nitric oxide synthase expression. *Journal of Neurochemistry*, *103*(5), 1872–1882. https://doi.org/10.1111/j.1471-4159.2007.04915.x

Martinowich, K., Manji, H., & Lu, B. (2007). New insights into BDNF function in depression and anxiety. *Nature Neuroscience*, *10*(9), 1089–1093.

McLaughlin, K. J., Gomez, J. L., Baran, S. E., & Conrad, C. D. (2007). The effects of chronic stress on hippocampal morphology and function: An evaluation of chronic restraint paradigms. *Brain Research*, *1161*, 56–64. https://doi.org/10.1016/j.brainres.2007.05.042

Mucha, M., Skrzypiec, A. E., Schiavon, E., Attwood, B. K., Kucerova, E., & Pawlak, R. (2011). Lipocalin-2 controls neuronal excitability and

anxiety by regulating dendritic spine formation and maturation. *Proceedings of the National Academy of Sciences of the United States of America*, *108*(45), 18436–18441.

Nguyen, C. H., & Watts, V. J. (2005). Dexras1 blocks receptor-mediated heterologous sensitization of adenylyl cyclase 1. *Biochemical and Biophysical Research Communications*, *332*, 913–920.

Ni, H. Y., Song, Y. X., Lin, Y. H., Cao, B., Wang, D. L., Zhang, Y., … Chang, L. (2018). Dissociating nNOS (neuronal NO synthase)-CAPON (carboxy-terminal postsynaptic density-95/discs large/zona occludens-1 ligand of nNOS) interaction promotes functional recovery after stroke via enhanced structural neuroplasticity. *Stroke*, *50*(3), 728–737.

Nicholson, B., & Verma, S. (2004). Comorbidities in chronic neuropathic pain. *Pain Medicine*, *5*(Suppl 1), S9–S27.

Sanacora, G., Zarate, C. A., Krystal, J. H., & Manji, H. K. (2008). Targeting the glutamatergic system to develop novel, improved therapeutics for mood disorders. *Nature Reviews. Drug Discovery*, *7*(5), 426–437.

Sareen, J., Cox, B. J., Afifi, T. O., de Graaf, R., Asmundson, G. J., ten Have, M., & Stein, M. B. (2005). Anxiety disorders and risk for suicidal ideation and suicide attempts: A population-based longitudinal study of adults. *Archives of General Psychiatry*, *62*, 1249–1257. https://doi.org/10.1001/archpsyc.62.11.1249

Soetanto, A., Wilson, R. S., Talbot, K., Un, A., Schneider, J. A., Sobiesk, M., … Arnold, S. E. (2010). Association of anxiety and depression with microtubule-associated protein 2- and synaptopodin-immunolabeled dendrite and spine densities in hippocampal CA3 of older humans. *Archives of General Psychiatry*, *67*(5), 448–457. https://doi.org/10.1001/archgenpsychiatry.2010.48

Song, M., Martinowich, K., & Lee, F. S. (2017). BDNF at the synapse: Why location matters. *Molecular Psychiatry*, *22*(10), 1370–1375. https://doi.org/10.1038/mp.2017.144

Vyas, A., Mitra, R., Shankaranarayana Rao, B. S., & Chattarji, S. (2002). Chronic stress induces contrasting patterns of dendritic remodeling in hippocampal and amygdaloid neurons. *The Journal of Neuroscience*, *22*(15), 6810–6818. https://doi.org/10.1523/JNEUROSCI.22-15-06810.2002

Wang, J. Q., & Mao, L. (2019). The ERK pathway: Molecular mechanisms and treatment of depression. *Molecular Neurobiology*, *56*(9), 6197–6205. https://doi.org/10.1007/s12035-019-1524-3

Warner-Schmidt, J. L., & Duman, R. S. (2006). Hippocampal neurogenesis: Opposing effects of stress and antidepressant treatment. *Hippocampus*, *16*(3), 239–249. https://doi.org/10.1002/hipo.20156

Xing, J., Ginty, D. D., & Greenberg, M. E. (1996). Coupling of the RAS-MAPK pathway to gene activation by RSK2, a growth factor-regulated CREB kinase. *Science*, *273*(5277), 959–963. https://doi.org/10.1126/science.273.5277.959

Xiong, H., Yamada, K., Han, D., Nabeshima, T., Enikolopov, G., Carnahan, J., & Nawa, H. (1999). Mutual regulation between the intercellular messengers nitric oxide and brain-derived neurotrophic factor in rodent neocortical neurons. *The European Journal of Neuroscience*, *11*(5), 1567–1576. https://doi.org/10.1046/j.1460-9568.1999.00567.x

Xu, B., Wratten, N., Charych, E. I., Buyske, S., Firestein, B. L., & Brzustowicz, L. M. (2005). Increased expression in dorsolateral prefrontal cortex of CAPON in schizophrenia and bipolar disorder. *PLoS Medicine*, *2*(10), e263. https://doi.org/10.1371/journal.pmed.0020263

Zhang, J., Huang, X. Y., Ye, M. L., Luo, C. X., Wu, H. Y., Hu, Y., … Zhu, D. Y. (2010). Neuronal nitric oxide synthase alteration accounts for the role of 5-HT1A receptor in modulating anxiety-related behaviors. *The Journal of Neuroscience*, *30*(7), 2433–2441. https://doi.org/10.1523/JNEUROSCI.5880-09.2010

Zhang, Y., Zhu, Z., Liang, H. Y., Zhang, L., Zhou, Q. G., Ni, H. Y., … Zhu, D. Y. (2018). nNOS-CAPON interaction mediates amyloid-β-induced neurotoxicity, especially in the early stages. *Aging Cell*, *17*(3), e12754. https://doi.org/10.1111/acel.12754

Zhou, L., Li, F., Xu, H. B., Luo, C. X., Wu, H. Y., Zhu, M. M., … Zhu, D. Y. (2010). Treatment of cerebral ischemia by disrupting ischemia-induced interaction of nNOS with PSD-95. *Nature Medicine*, *16*(12), 1439–1443. https://doi.org/10.1038/nm.2245

Zhou, L., & Zhu, D. Y. (2009). Neuronal nitric oxide synthase: Structure, subcellular localization, regulation, and clinical implications. *Nitric Oxide*, *20*(4), 223–230. https://doi.org/10.1016/j.niox.2009.03.001

Zhou, Q. G., Hu, Y., Hua, Y., Hu, M., Luo, C. X., Han, X., … Zhu, D. Y. (2007). Neuronal nitric oxide synthase contributes to chronic stress-induced depression by suppressing hippocampal neurogenesis. *Journal of Neurochemistry*, *103*(5), 1843–1854. https://doi.org/10.1111/j.1471-4159.2007.04914.x

Zhou, Q. G., Zhu, L. J., Chen, C., Wu, H. Y., Luo, C. X., Chang, L., & Zhu, D. Y. (2011). Hippocampal neuronal nitric oxide synthase mediates the stress-related depressive behaviors of glucocorticoids by down-regulating glucocorticoid receptor. *The Journal of Neuroscience*, *31*(21), 7579–7590. https://doi.org/10.1523/JNEUROSCI.0004-11.2011

Zhou, Q. G., Zhu, X. H., Nemes, A. D., & Zhu, D. Y. (2018). Neuronal nitric oxide synthase and affective disorders. *IBRO Rep*, *5*, 116–132. https://doi.org/10.1016/j.ibror.2018.11.004

Zhu, L. J., Li, T. Y., Luo, C. X., Jiang, N., Chang, L., Lin, Y. H., … Zhu, D. Y. (2014). CAPON-nNOS coupling can serve as a target for developing new anxiolytics. *Nature Medicine*, *20*(9), 1050–1054. https://doi.org/10.1038/nm.3644

Zhu, L. J., Ni, H. Y., Chen, R., Chang, L., Shi, H. J., Qiu, D., … Zhu, D. Y. (2018). Hippocampal nuclear factor kappa B accounts for stress-induced anxiety behaviors via enhancing neuronal nitric oxide synthase (nNOS)-carboxy-terminal PDZ ligand of nNOS-Dexras1 coupling. *Journal of Neurochemistry*, *146*(5), 598–612. https://doi.org/10.1111/jnc.14478

## SUPPORTING INFORMATION

Additional supporting information may be found online in the Supporting Information section at the end of this article.